

A peer-reviewed version of this preprint was published in PeerJ on 25 April 2016.

[View the peer-reviewed version](https://peerj.com/articles/1973) (peerj.com/articles/1973), which is the preferred citable publication unless you specifically need to cite this preprint.

Doblin MA, Petrou K, Sinutok S, Seymour JR, Messer LF, Brown MV, Norman L, Everett JD, McInnes AS, Ralph PJ, Thompson PA, Hassler CS. 2016. Nutrient uplift in a cyclonic eddy increases diversity, primary productivity and iron demand of microbial communities relative to a western boundary current. PeerJ 4:e1973
<https://doi.org/10.7717/peerj.1973>

Nutrient uplift in a cyclonic eddy increases diversity, primary productivity and iron demand of microbial communities relative to a western boundary current

Martina A Doblin, Katherina Petrou, Sutinee Sinutok, Justin R Seymour, Lauren F Messer, Mark V Brown, Louiza Norman, Jason D Everett, Allison S McInnes, Peter J Ralph, Peter A Thompson, Christel S Hassler

The intensification of western boundary currents in the global ocean will potentially influence meso-scale eddy generation, and redistribute microbes and their associated ecological and biogeochemical functions. To understand eddy-induced changes in microbial community composition as well as how they control growth, we targeted the East Australian Current (EAC) region to sample microbes in a cyclonic (cold-core) eddy (CCE) and the adjacent EAC. Phototrophic and diazotrophic microbes were more diverse (2 to 10 times greater Shannon index) in the CCE relative to the EAC, and the cell size distribution in the CCE was dominated (67%) by larger micro-plankton ($\geq 20 \mu\text{m}$), as opposed to pico- and nano-sized cells in the EAC. Nutrient addition experiments determined that nitrogen was the principal nutrient limiting growth in the EAC, while iron was a secondary limiting nutrient in the CCE. Among the diazotrophic community, heterotrophic *NifH* gene sequences dominated in the EAC and were attributable to members of the gamma-, beta-, and delta-proteobacteria, while the CCE contained both phototrophic and heterotrophic diazotrophs, including *Trichodesmium*, UCYN-A and gamma-proteobacteria. Daily sampling of incubation bottles following nutrient amendment captured a cascade of effects at the cellular, population and community level, indicating taxon-specific differences in the speed of response of microbes to nutrient supply. Nitrogen addition to the CCE community increased picoeukaryote chlorophyll *a* quotas within 24 h, suggesting that nutrient uplift by eddies causes a 'greening' effect as well as an increase in phytoplankton biomass. After three days in both the EAC and CCE, diatoms increased in abundance with macronutrient (N, P, Si) and iron amendment, whereas haptophytes and phototrophic dinoflagellates declined. Our results indicate that cyclonic eddies increase delivery of nitrogen to the upper ocean to potentially mitigate the negative consequences of increased stratification due to ocean warming, but also increase the biological demand for iron that is necessary to sustain the growth of large-celled phototrophs and potentially support the diversity of diazotrophs over longer time-scales.

1 **Nutrient uplift in a cyclonic eddy increases diversity, primary productivity and iron**
2 **demand of microbial communities relative to a western boundary current**

3
4 M.A. Doblin¹, K. Petrou², S. Sinutok^{1,3}, J. Seymour¹, L.F. Messer¹, M.V. Brown⁴, L. Norman^{1,5},
5 J.D. Everett⁶, A. McInnes¹, P. J. Ralph¹, P.A. Thompson⁷, C. Hassler⁸

6 1. Plant Functional Biology and Climate Change Cluster, University of Technology Sydney,
7 Ultimo, NSW, Australia

8 2. School of Life Sciences, University of Technology Sydney, Ultimo, NSW, Australia

9 3. Faculty of Environmental Management, Prince of Songkla University, Kho Hong, Songkhla
10 90112, Thailand

11 4. School of Biotechnology and Biomolecular Sciences, University of New South Wales,
12 Randwick, NSW, Australia

13 5. Department of Plant Sciences, University of Cambridge, Cambridge, United Kingdom

14 6. School of Biological, Earth and Environmental Sciences, University of New South Wales,
15 Randwick, NSW, Australia

16 7. Oceans and Atmosphere Flagship, Commonwealth Scientific Industrial Research
17 Organisation, , Hobart , Australia.

18 8. Institute F.-A. Forel, Earth and Environmental Sciences, University of Geneva, Geneva,
19 Switzerland

20

21

22 Corresponding author:

23 Martina Doblin

24 Plant Functional Biology and Climate Change Cluster, University of Technology Sydney,
25 Thomas Street, Ultimo, NSW, 2007, Australia

26 Martina.Doblin@uts.edu.au

27

28 **Abstract**

29 The intensification of western boundary currents in the global ocean will potentially influence
30 meso-scale eddy generation, and redistribute microbes and their associated ecological and
31 biogeochemical functions. To understand eddy-induced changes in microbial community
32 composition as well as how they control growth, we targeted the East Australian Current (EAC)
33 region to sample microbes in a cyclonic (cold-core) eddy (CCE) and the adjacent EAC.
34 Phototrophic and diazotrophic microbes were more diverse (2 to 10 times greater Shannon
35 index) in the CCE relative to the EAC, and the cell size distribution in the CCE was dominated
36 (67%) by larger micro-plankton ($\geq 20 \mu\text{m}$), as opposed to pico- and nano-sized cells in the EAC.
37 Nutrient addition experiments determined that nitrogen was the principal nutrient limiting
38 growth in the EAC, while iron was a secondary limiting nutrient in the CCE. Among the
39 diazotrophic community, heterotrophic *NifH* gene sequences dominated in the EAC and were
40 attributable to members of the gamma-, beta-, and delta-proteobacteria, while the CCE contained
41 both phototrophic and heterotrophic diazotrophs, including *Trichodesmium*, UCYN-A and
42 gamma-proteobacteria. Daily sampling of incubation bottles following nutrient amendment
43 captured a cascade of effects at the cellular, population and community level, indicating taxon-
44 specific differences in the speed of response of microbes to nutrient supply. Nitrogen addition to
45 the CCE community increased picoeukaryote chlorophyll *a* quotas within 24 h, suggesting that
46 nutrient uplift by eddies causes a ‘greening’ effect as well as an increase in phytoplankton
47 biomass. After three days in both the EAC and CCE, diatoms increased in abundance with
48 macronutrient (N, P, Si) and iron amendment, whereas haptophytes and phototrophic
49 dinoflagellates declined. Our results indicate that cyclonic eddies increase delivery of nitrogen to
50 the upper ocean to potentially mitigate the negative consequences of increased stratification due
51 to ocean warming, but also increase the biological demand for iron that is necessary to sustain

52 the growth of large-celled phototrophs and potentially support the diversity of diazotrophs over
53 longer time-scales.

54

55

56

57

59 Introduction

60 There are two broad nutrient limitation regimes for phytoplankton growth in the contemporary
61 ocean, whereby iron (Fe) limitation occurs across ~30% of the ocean's surface area where high
62 macronutrient concentrations occur (high latitudes, upwelling and some coastal areas), and
63 nitrogen (N) limitation occurs across most of the oligotrophic low-latitude systems (Moore et al.
64 2013). Different phytoplankton groups can have specific nutrient requirements, such as Fe for
65 diazotrophs (Kustka et al 2003) and silicon (Si) for diatoms (Brzezinski & Nelson 1989), which
66 may lead to secondary or interactive effects on Fe or N limitation. Co-limitation may also arise
67 when there is physical mixing between water masses with different nutrient stoichiometry, or
68 over seasonal cycles when physical nutrient inputs and biological cycling alters nutrient
69 bioavailability (Deutsch & Weber 2012).

70 Global Climate Model (GCM) projections indicate warming and increased stratification of the
71 upper ocean over the coming decades, limiting the upwards delivery of nitrogen (e.g., "new" N)
72 into the euphotic zone, and potentially leading to increased reliance on a smaller pool of
73 regenerated forms or N fixation to support primary production (Behrenfeld 2011). However,
74 these models typically do not consider the influence of smaller scale oceanographic features such
75 as meso-scale eddies, which could act as a compensatory mechanism and enrich the upper ocean
76 with new nutrients delivered from deeper ocean waters, potentially mitigating the negative
77 consequences of climate change (Matear et al. 2013).

78 While eddies are universal features of the global ocean (Chelton, Schlax & Samelson 2011), they
79 differ in their mode of formation, direction of rotation, size, longevity, and processes driving
80 nutrient dynamics (e.g. interaction between wind and surface currents, horizontal entrainment;

81 Gaube et al. 2014), and can thus have different biological effects (Bibby et al. 2008). Eddies
82 formed in coastal regions, for example, can entrain enriched continental shelf water (Waite et al.
83 2007), and consequently have higher positive chlorophyll-a anomalies than their oceanic
84 counterparts (Everett et al. 2012). The ratio of upwelled nutrients (e.g., Si:N) delivered into the
85 euphotic zone is also important in determining the structure of microbial communities sustained
86 by eddies and influences their biogeochemical function (Bibby & Moore 2011). Therefore, the
87 role eddies play in regulating internal nutrient inputs from the deep ocean is likely to be
88 regionally dependent.

89 Much of what is known about eddies and their impact on the base of the foodweb is derived from
90 satellite ocean colour observations which provide limited information with respect to microbial
91 species composition and biogeochemical activity, and have a restricted view of the upper ocean
92 (McGillicuddy 2016). *In situ* observations and manipulative experiments are therefore critical to
93 develop a full understanding of the role of meso-scale eddies in upper-ocean ecosystem
94 dynamics and biogeochemical cycling.

95 Australia has one of the longest north-south coastlines in the world, and the oceanography along
96 its east coast is extremely dynamic. It is strongly influenced by the flow of the Eastern Australian
97 Current (EAC), one of five western boundary currents (WBCs) in the global ocean. Southward of
98 $\sim 32^\circ\text{S}$ 153°E , where two thirds of the EAC deviates eastward towards New Zealand to form the
99 Tasman Front, the remaining EAC flow meanders, breaking down into a complex series of meso-
100 scale eddies (Ridgway & Godfrey, 1997). The number and frequency of these eddies is higher
101 than in the broader Tasman Sea, and their biological properties differentiate more strongly from
102 background ocean waters than their oceanic counterparts (Everett et al. 2014). A critical research
103 question is whether the observed intensification of the EAC (Wu et al., 2012) will result in more

104 eddies, a change in the nature of these eddies, and how they will impact on primary producers
105 and higher trophic levels.

106 Given that offshore phytoplankton communities in the Tasman Sea are generally N limited
107 (Hassler et al. 2011; Ellwood et al. 2013), and that cyclonic cold-core eddies displace isopycnal
108 surfaces (seawater of similar density) upwards and can upwell nutrients into the euphotic zone
109 (McGillicuddy et al., 1998), EAC-induced eddies could increase the supply of nitrogen into
110 surface waters from below the thermocline and potentially alter controls on phytoplankton
111 growth. However, another source of N into surface waters is from N₂ fixing microbes. At least
112 four different groups of diazotrophs have been identified from Australian waters: the
113 filamentous, photosynthetic cyanobacterium *Trichodesmium*, the unicellular phycoerythrin-
114 containing cyanobacterium *Crocospaera watsonii* (group B), the photoheterotrophic symbiont
115 UCYN-A (associated with specific prymnesiophyte hosts; Hagino et al. 2013), and heterotrophic
116 proteobacteria (Moisander et al. 2010; Seymour et al. 2012; Messer et al. 2015). The regional
117 distribution of diazotrophs in the western South Pacific suggests there is a sufficient supply of Fe
118 to satisfy the requirements of the nitrogenase enzyme (Kustka et al 2003), but little is known
119 about how eddies may change the delivery of Fe or N from depth in this region, and hence alter
120 the dynamics of diazotrophs relative to other microbial groups.

121 This study targeted the western Tasman Sea, which is dominated by the East Australian Current
122 (EAC) and its associated eddy field. We examined the composition and diversity of the microbial
123 community in a cyclonic cold core eddy (CCE) and in the EAC, and examined their responses to
124 separate additions of nitrate (N), nitrate with iron (NFe), silicic acid (Si) as well as a mix of
125 nutrients containing N, Fe, Si and phosphate (P). We focused on communities from the
126 subsurface chlorophyll-a maximum to simulate the impact of moderate nutrient uplift into the

127 euphotic zone (i.e., upwelling that does not reach the surface), and advance knowledge about
128 responses of microbial communities that are difficult to detect using satellites.

129

130 **Materials and Methods**

131 **Study site and water collection.** The experiments were conducted on the *RV Southern Surveyor*
132 during austral spring in 2010 (15 - 31 October) between 29 and 36 °S, and 150 and 155 °E (Fig.
133 1A). Sampling sites were chosen with the assistance of daily Moderate Resolution Imaging
134 Spectroradiometer (MODIS) and Advanced Very High Resolution Radiometer (AVHRR)
135 satellite imagery and targeted the EAC and a meso-scale cyclonic (cold core) eddy (CCE; Fig.
136 1B). To examine the oceanographic context of the sampling period, MODIS Level 3 sea-surface
137 temperature was obtained from the Integrated Marine Observing System (IMOS) Data
138 Portal (<http://imos.aodn.org.au/imos/>) at 1 km resolution. Satellite altimeter data were obtained
139 from NASA/CNES (Jason-1 and 2) and ESA (ENVISAGE) via the IMOS portal.

140

141 At each site, the physico-chemical properties of the water column (0 – 200 m) were measured
142 with the aid of a Conductivity-Temperature-Depth (CTD; Seabird SBE911-plus) equipped with a
143 fluorometer (AquaTracker Mk3, Chelsea, UK), transmissometer (Wetlabs C-Star (25cm optical
144 path)), dissolved oxygen (Seabird SBE43) and Photosynthetically Active Radiation (PAR;
145 Biospherical Instruments QCP-2300 Log Quantum Cosine Irradiance Sensor) sensor.

146 Seawater used to assess microbial composition and diversity, as well as for nutrient amendment
147 experiments was collected from the depth of the chlorophyll *a* (Chl-*a*) fluorescence maximum
148 (as determined by the down-cast fluorescence profile) using 10 L Niskin bottles (80 m in the
149 EAC, and 41 m in the CCE). A trace metal clean rosette was not available for this voyage, so the

150 following precautions were taken to minimise trace metal contamination. Water was sampled
151 from Niskin bottles through acid washed silicon tubing with plastic bags covering the tubing and
152 bottle neck, and polyethelene gloves were worn during water sampling and manipulation.
153 Seawater was filtered through acid-soaked 200-210 μm mesh to remove mesozooplankton
154 grazers and collected in 20 L acid washed (1 N HCl, rinsed 7-times with MilliQ water) LDPE or
155 PC carboys. Carboys were stored in double-plastic bags and kept in plastic boxes to avoid
156 contact with the ship. All subsequent sampling took place in a custom-made, metal free laminar
157 flow cabinet, dedicated for trace metal clean work using standard clean room procedures.

158 **Experimental setup.** Water was homogenised, sampled for dissolved nutrients, flow cytometry,
159 phytoplankton pigments, nucleic acid collection and photo-physiological measurements, with the
160 remainder transferred into pre-treated acid washed (1 N HCl, rinsed 7-times with MilliQ water) 4
161 L polycarbonate bottles (Nalgene) under laminar flow conditions. Bottles were randomly
162 allocated to five nutrient addition treatments in triplicate: an unamended control, +NO₃ (10 μM
163 nitrate final concentration), +NO₃+FeCl₃ (10 μM and 1 nM final concentration (ICP-MS 1g/L
164 standard, Fluka), respectively), +Si(OH)₄ (10 μM final concentration), nutrient mix
165 (+NO₃+Si+PO₄+Fe; 10N : 10Si : 0.625P μM in Redfield proportions and 1 nM Fe respectively).
166 After the addition of nutrients, bottles were capped, gently inverted and lids sealed with parafilm,
167 before being placed into an on-deck, flow-through incubator, exposed to 25 % surface irradiance
168 and in situ temperature conditions. Surface seawater supplying the deck board incubators was
169 21.94 ± 0.47 during the EAC incubation and 21.57 ± 0.27 during the CCE incubations. This
170 closely matches the *in situ* temperature for both EAC (80 m) and CCE (41 m) communities at the
171 time of sampling (Table 1).

172 For the EAC experiment, control bottles were sampled daily for maximum quantum yield of
173 photosystem II (F_V/F_M) before being enriched with their respective nutrient or nutrient mix
174 treatment, then re-sealed and returned to the on-deck incubator. The same sampling protocol was
175 used in the CCE; however, no additional nutrient additions were made after the initial
176 amendment to avoid accumulation of excess nutrients. To limit nutrient or microbiological cross-
177 contamination, the same bottles were re-used for identical experimental (nutrient) treatments
178 across the EAC and CCE experiments. Macronutrient analyses were carried out on board by
179 CSIRO Marine and Atmospheric Research (CMAR) according to Cowley et al. (1999). Nutrient
180 measurements had a standard error $< 0.7\%$ and a detection limit of $0.035\ \mu\text{M}$ for NO_x , $0.012\ \mu\text{M}$
181 for Si and $0.009\ \mu\text{M}$ for PO_4 .

182 After 3 days (72 - 78 h) of incubation, nutrient experiments were terminated. Microbial
183 responses to nutrient additions were quantified by measuring pigments (Chl-a and other
184 accessory pigments), abundance of pico- and nano-phytoplankton and heterotrophic bacteria via
185 flow cytometry, and DNA sequencing for characterising prokaryote and diazotroph community
186 diversity and composition (16S ribosomal RNA, nitrogenase *NifH* subunit targeted,
187 respectively).

188 **Pigment Analysis.** Seawater (minimum volume 2.2 L) was filtered under low vacuum (e.g. \leq
189 $100\ \text{mm Hg}$) onto 25 mm GF/F filters in low light ($< 10\ \mu\text{mol photons m}^{-2}\ \text{s}^{-1}$). Filters were
190 folded in half, blotted dry on absorbent paper, placed into screw-capped cryovials and stored in
191 liquid nitrogen until pigment analysis. In the laboratory, pigments were extracted and analysed
192 using High Performance Liquid Chromatography (HPLC) as described in Hassler et al. (2011).
193 Biomarker pigments were used to infer the distribution of dominant phototrophs. Each biomarker
194 pigment was normalised against chlorophyll-a (the universal pigment in all phytoplankton) to

195 account for spatial variation in the total phytoplankton biomass. Briefly, biomarkers represent the
196 following phytoplankton groups: Zeaxanthin (Zea) = cyanobacteria; 19'Hexanoyloxyfucoxanthin
197 (19-Hex) = haptophytes; Chlorophyll b (Chl-b) and lutein = Chlorophytes; Alloxanthin (Allo) =
198 cryptophytes, 19'Butanoloxyfucoxanthin (19-But) = pelagophytes; Prasinoloxanthin (Prasino) =
199 prasinophytes; Peridinin (Per) = autotrophic dinoflagellates; and Fucoxanthin (Fuco) = diatoms,
200 prymnesiophytes, chrysophytes, pelagophytes and raphidophytes. The photosynthetic (PSC) and
201 photoprotective (PPC) carotenoid pigment contributions were calculated as in Barlow et al.
202 (2007), and the approach of Uitz et al. (2008) was used to assess the taxonomic composition of
203 the phytoplankton community and characterise its size structure. While this method may be
204 subject to error because pigments are shared between different phytoplankton groups, and some
205 groups are spread across different sizes, we apply it in this study to examine relative (not
206 absolute) differences in size structure between water masses and nutrient treatments.

207 **Flow Cytometry.** Samples for enumeration of pico- and nano-phytoplankton were fixed with
208 glutaraldehyde (1% v/v final concentration), snap frozen in liquid nitrogen and stored at -80° C.
209 Populations of *Prochlorococcus*, *Synechococcus* and picoeukaryotes were discriminated using
210 side scatter (SSC) and red and orange fluorescence (Marie et al. 1997) using a flow cytometer
211 (LSR II, BD Biosciences). Pigment content per cell was normalised to the fluorescence of
212 standard yellow-green beads (1 µm FluoSpheres®, Life Technologies) that were added to each
213 sample immediately before analysis. Samples for bacterial analysis were stained with SYBR
214 Green I nucleic acid stain (1:10000 final dilution; Molecular Probes) (Marie et al. 1997) and high
215 and low nucleic acid content populations were discriminated according to green fluorescence and
216 side scatter properties (Gasol & Del Giorgio 2000; Seymour, Seuront & Mitchell 2007). Data
217 was analysed using Cell-Quest Pro (BD Biosciences).

218 **DNA extraction and sequence analysis of prokaryote and diazotrophic communities.**

219 Water samples (2 L) for DNA analyses were filtered onto 0.2 µm polycarbonate membrane
220 filters (Millipore), snap frozen in liquid nitrogen and stored at -80 °C prior to analysis. Genomic
221 DNA was subsequently extracted using the Power Water DNA extraction kit (MoBio
222 Laboratories, Inc) following the manufacturer's protocols and DNA concentration was quantified
223 using a Qubit® 2.0 fluorometer (Invitrogen). To determine bacterial community composition, the
224 V1-V3 region of the 16S rRNA gene was amplified using the primer sets in Table S1, and
225 sequenced by 454 pyrosequencing (Roche, FLX Titanium; Molecular Research LP) following
226 previously published protocols (Acosta-Martínez et al. 2008; Dowd et al. 2008). 16S rRNA gene
227 sequences were analysed and processed using the Quantitative Insights into Microbial Ecology
228 software (QIIME; Caporaso et al. 2010). Briefly, samples were quality filtered, de-multiplexed
229 and clustered based on 97 % sequence identity using UCLUST (Edgar 2010). Taxonomy was
230 assigned according to the latest version of the SILVA database (111; Quast et al. 2013) and
231 samples were rarefied to the lowest number of sequences to ensure even sampling effort across
232 samples (14,621 sequences per sample).

233 For N₂-fixing bacteria, the gene encoding a subunit of the enzyme nitrogenase (*NifH*, Zehr,
234 Mellon & Hiorns 1997; Zehr et al. 2003) was amplified and sequenced from genomic DNA
235 using previously published methods (Zehr & McReynolds 1989; Zehr & Turner 2001). A nested
236 PCR protocol was used to amplify an approximately 359 bp region of the *NifH* gene using two
237 sets of degenerate primers listed in Table S1. PCR products were purified using the Ultra Clean
238 PCR Clean-up Kit (MoBio Laboratories, Inc) following the manufacturer's instructions. The
239 *nifH* amplicons were sequenced by 454 pyrosequencing (Roche, FLX Titanium; Molecular
240 Research LP) after an additional 10-cycles PCR with custom barcoded NifH1 and NifH2 primers

241 under the same reaction conditions (Dowd et al. 2008; Farnelid et al. 2011, 2013). Raw
242 sequences were quality filtered, and de-multiplexed in QIIME (Caporaso et al. 2010). Sequences
243 were clustered at 95 % sequence identity using UCLUST, whereby *nNifH* sequences within 5%
244 identity of a centroid read were assigned as operational taxonomic units (OTUs) (Edgar 2010),
245 then rarefied to 1,050 sequences per sample to ensure even sampling effort, resulting in 989 *NifH*
246 OTUs. Since many of these *NifH* OTUs were singletons, only OTUs with ≥ 100 sequences
247 assigned to them were analysed further (representing 85 % of total *NifH* sequences), resulting in
248 16 OTUs. Putative taxonomy was assigned using BLASTn (Altschul et al. 1990) against the
249 NCBI Nucleotide collection database, and translated *NifH* sequences were compared to the
250 Ribosomal Database Project's *NifH* protein database using FrameBot (Wang et al. 2013; Fish et
251 al. 2013).

252 **Photophysiological measurements.** Photosynthetic efficiency of microbial phototrophs was
253 measured using a Pulse Amplitude Modulated (PAM) fluorometer (Water-PAM; Walz GmbH,
254 Effeltrich, Germany). A 3 ml aliquot of water was transferred to a quartz cuvette and after a 10
255 min dark-adaptation period, minimum fluorescence (F_0) was recorded. Upon application of a
256 saturating pulse of light (pulse duration = 0.8 s; pulse intensity $>3000 \mu\text{mol photons m}^{-2} \text{s}^{-1}$)
257 maximum fluorescence (F_M) was determined. From these two parameters, F_v/F_M was calculated
258 according to the equation $(F_M - F_0)/F_M$ (Schreiber 2004).

259 **Phytoplankton primary production measurements.** Phytoplankton primary production was
260 estimated at the end of the 3-day experiments using small volume ^{14}C incubations as described in
261 Doblin et al. (2011). Carbon uptake rates were normalised to *in situ* chlorophyll *a* concentrations.
262 Carbon fixation-irradiance relationships were then plotted and the equation of Platt, Gallegos &
263 Harrison(1980) used to fit curves to data using least squares non-linear regression.

264 Photosynthetic parameters included light-saturated photosynthetic rate [P_{\max} , mg C (mg Chl-a)⁻¹
265 h⁻¹], initial slope of the light-limited section of the carbon fixation-irradiance curve [α , mg C (mg
266 Chl-a)⁻¹ h⁻¹ ($\mu\text{mol photons m}^{-2} \text{s}^{-1}$)⁻¹], and light intensity at which carbon-uptake became maximal
267 (calculated as $P_{\max}/\alpha = E_k$, $\mu\text{mol photons m}^{-2} \text{s}^{-1}$).

268 **Statistical analysis.** Differences in microbial composition and diversity between the initial EAC
269 and CCE communities, and between nutrient treatments within each water mass were assessed
270 using analysis of variance (ANOVA; $\alpha = 0.05$). Data were analysed comparing responses at the
271 end of incubation, t_{72} (72 - 78 h), across treatments, as well as comparing the differences over
272 time from the initial water (t_0) to t_{72} . Multiple comparison adjustment of the p-value was made
273 using a Tukey's HSD test. To ensure that the assumption of equal variances for all parametric
274 tests was satisfied, a Levene's test for homogeneity of variance was applied to all data *a priori*
275 and when necessary, data was transformed. All analyses were performed using SPSS statistical
276 software (version 22, IBM, New York USA).

277 To examine overall changes in microbial assemblages due to nutrient amendment, composition
278 data (i.e. for phototrophs, diagnostic pigments standardised to total Chl-a, flow cytometric
279 counts; for heterotrophs and diazotrophs, rarefied 16S and *NifH* sequence data, respectively)
280 were square root transformed and a resemblance matrix was generated using Bray-Curtis
281 similarity in the PRIMER software package (Clarke & Warwick 2001). Analysis of similarities
282 (ANOSIM) was used to test the hypothesis that different nutrient amendments would influence
283 microbial composition (Clarke 1993). The contribution of phytoplankton groups to the observed
284 significant differences in community assemblage, as a function of treatment, were determined
285 using Similarity Percentage Analysis (SIMPER; Clarke 1993).

286

287 **Results**

288 **Oceanographic setting.** During the voyage, the EAC was flowing southward along the
289 continental shelf edge (Fig. 1B) with a core surface temperature of 23-24 °C. The EAC surface
290 velocity was 1.2 m s⁻¹ estimated from altimetry (Fig. 1B, arrows) with the current separating
291 from the coast at ~ 30 °S, forming the Tasman Front. The EAC station (Fig. 1B) had a
292 temperature range of 21.4 to 22.5 °C and a salinity of 35.45 to 35.52 in the upper 200 m of the
293 water-column. The cyclonic eddy, south of the EAC station, was sampled on 25th October 2015
294 when it centred at 32 °S adjacent to the continental shelf. The CCE had a temperature range of
295 14.3 to 21.8 °C and a salinity of 35.26 to 35.54 in the upper 200 m of the water-column.

296 Dissolved macronutrient stocks indicated the potential for widespread N limitation in the EAC
297 and adjacent shelf and Tasman Sea (offshore) waters (Fig. 2A), with nitrate deficit ($N^* = [NO_3^-]$
298 $- 16[PO_4^{3-}]$) occurring to at least 200 m (overall mean for all depths \pm SD = $-1.9 \pm 0.53 \mu M$; Fig.
299 2B). Oxidised N (nitrate) was detectable at the Chl-a fluorescence maximum in the EAC (80 m)
300 and CCE (41 m), ranging between 0.1 and 0.3 μM (Fig. 3), with dissolved phosphate being ~0.1
301 μM in both water masses (Table 1).

302 **Microbial community composition and diversity in different water masses.** Initial Chl-a
303 concentrations were relatively low (0.106 and 0.336 $\mu g L^{-1}$), but distinct (p-value < 0.05), in the
304 EAC and CCE, respectively (Table 1; t0 Fig. 4A and B). The most abundant phototroph in the
305 EAC was the cyanobacterium *Prochlorococcus*, whereas in the CCE it was *Synechococcus* (Fig.
306 S1). A significant proportion of larger phototrophs in the EAC contained 19'-
307 hexanoyloxyfucoxanthin (Hex-Fuco; t0 Fig 4E), exclusively found in haptophytes, including the
308 coccolithophores (Liu et al. 2009). However, in the CCE, fucoxanthin (found in Phaeophyta and
309 most other heterokonts), was the dominant accessory pigment, largely indicative of diatoms (t0

310 Fig. 4D). Pigment ratios suggested the size structure of the EAC phototrophic community was
311 dominated by pico- and nano-plankton ($< 2 \mu\text{m}$) and in the CCE by microplankton ($\geq 20 \mu\text{m}$; t0
312 Fig. 5A and B, respectively). Pigment richness was 30% higher in the CCE than in the EAC, and
313 phototrophic alpha-diversity was ~40% higher (Shannon's index calculated using HPLC pigment
314 data = 1.02 ± 0.05 compared to 0.64 ± 0.02 in the EAC; average \pm SD here and throughout).

315 With respect to the heterotrophs, the total abundance of bacteria was similar in both water
316 masses ($\sim 8.5 \times 10^5$ cells ml^{-1} ; t0 Fig. 5I and J) but there was a greater proportion of high DNA
317 bacteria in the CCE (47 ± 4 vs 39 ± 2 % in the EAC). The greatest proportion of bacterial 16S
318 rRNA sequences in both water masses belonged to the alpha-proteobacteria (SAR11 and
319 SAR116 clade), Rhodobacteriaceae, as well as *Synechococcus* and *Prochlorococcus* (Fig. 6) but
320 there was no difference in bacterial alpha-diversity between water masses (Shannon's index in
321 EAC = 3.20 ± 0.13 compared to 3.10 ± 0.19 in the CCE). Heterotrophic *NifH* gene sequences
322 were detected in the EAC and were primarily attributable to members of the gamma-, beta-, and
323 delta-proteobacteria. Initial CCE samples were not available (cryovials broken in storage);
324 however control CCE treatments contained phototrophic and heterotrophic diazotrophs,
325 including *Trichodesmium*, UCYN-A and gamma-proteobacterial *NifH* sequences.

326 **Nutrient-induced shifts in the phototrophic community.** After 3 days, there was a large
327 positive effect of NFe and the nutrient Mix (N,P,Si,Fe) on the total Chl-a concentration in the
328 EAC community (Fig. 4A), which occurred alongside an increase in fucoxanthin relative to Chl a
329 in the NFe and Mix treatments (p-value ≤ 0.026 ; Fig. 4C), suggesting a greater relative
330 abundance of diatoms (Table 2). The relative abundance of haptophytes (as indicated by pigment
331 Hex-Fuco) showed a declining trend across all treatments, but by the end of the experiment
332 haptophytes were least abundant in the NFe treatment (p-value ≤ 0.031 ; Fig. 4E).

333 *Prochlorococcus* (as determined by flow cytometric counts) decreased in all treatments including
334 the controls (Fig. 5G), but *Synechococcus* abundance declined only in the Mix treatment (Fig.
335 5E). Collectively, there was a decrease in picoeukaryote abundance in all but the NFe EAC
336 bottles by day 3 (p-value < 0.05; Table 2), with the phototrophic community overall showing a
337 significant cell size increase into the micro size class (nominally $\geq 20 \mu\text{m}$) with N amendment
338 (p-value < 0.05; Fig. 5A), as estimated through pigment ratios (Uitz et al. 2008). Taken as a
339 whole, the largest shift in phototrophic community composition and structure was in the mix
340 treatment relative to all other treatments (SIMPER, >75% dissimilarity), which was attributed
341 mainly to the decrease in picoeukaryotes. Importantly, the EAC community was more similar to
342 the t_0 CCE community after nutrient amendment, particularly with NFe addition (Global R =
343 0.48, p-value < 0.05; Fig 7C).

344 In contrast, within the CCE, addition of N, NFe and Mix caused a significant increase in Chl-a
345 relative to the initial community (Fig. 4B; Table 2). Consistent with the patterns seen in the
346 EAC, Fucoxanthin:Chl-a increased in NFe and Mix bottles (and in the N treatment), which was
347 concomitant with a decline in haptophytes (Hexo-Fuco:Chl-a; Fig. 4D and F; Table 2). There
348 was a decrease in picoeukaryotes in the Mix treatment relative to unamended controls (Fig. 5D),
349 as well as a measurable increase in *Prochlorococcus* with NFe amendment (Fig. 5H).
350 *Synechococcus* showed little effect of nutrient amendment in the CCE but declined when all
351 nutrients were added together (p-value < 0.05; Fig. 5F; Table 2). Similar to the EAC, there was
352 an overall increase in cell size of the CCE phototrophic assemblage into the micro size class with
353 NFe and Mix amendment (p-value < 0.05; Fig. 5B). The Mix addition caused the greatest shift in
354 cell size structure, decreasing the abundance of small cells by an order of magnitude (Fig. 5).
355 Similar to the EAC community, the largest shift in phototrophic community composition and

356 structure was in the Mix relative to all other treatments (SIMPER, $\geq 55\%$ dissimilarity), mainly
357 due to the decrease in *Synechococcus* and picoeukaryotes.

358 **Nutrient-induced shifts in the heterotrophic community.** Nutrient-induced changes in the
359 EAC bacterioplankton community were also detected by the end of the experiment (Figs. 5I, 6,
360 7). There was a significant (but relatively small) decrease in the relative abundance of sequences
361 matching SAR11 Surface 1 and SAR116 clades, and an increase in relative abundance of
362 *Synechococcus* with N, NFe, Mix addition, with the greatest dissimilarity in bacterial community
363 composition observed between the t_0 and NFe treatments (SIMPER, 29 % dissimilarity). These
364 shifts in SAR11, SAR116 and *Synechococcus* relative abundance contributed to 3, 2 and 2 %
365 dissimilarity between the t_0 and NFe treatments respectively (Fig.6; SIMPER). This pattern of
366 increasing *Synechococcus* sequence abundance was consistent with the patterns of
367 *Synechococcus* abundance revealed from flow cytometry (Fig. 5E). Within EAC nutrient
368 addition treatments, the greatest dissimilarity was observed between bacterioplankton
369 communities in the NFe and Si amendments (SIMPER, 29 % dissimilarity). A relative decrease
370 in *Synechococcus* with Si, and an increase in the SAR116 clade and *Prochlorococcus*,
371 contributed 3, 2 and 2 % to the dissimilarity between NFe and Si treatments, respectively (Fig. 6;
372 SIMPER).

373 In the CCE bacterioplankton composition was distinct from the EAC in unamended controls
374 after 3 days (ANOSIM, Global R: 1.00, p-value < 0.01 ; Fig. 7F), with the SAR116 clade and
375 Rhodobacteraceae more abundant in the CCE than in the EAC, and SAR11 surface clade and
376 *Prochlorococcus* less abundant (Fig. 6. Total heterotrophic bacterial abundance in the CCE
377 doubled after 3 days with Si and Mix addition, unlike the EAC community (Fig. 5I and J).

378 However, there was no appreciable shift in bacterioplankton diversity between nutrient addition
379 treatments (Fig. 7E; ANOSIM, Global R: 0.14, p-value > 0.05).

380 Similar to the patterns observed in the overall bacterioplankton composition, diazotroph diversity
381 in the EAC shifted following nutrient amendment (ANOSIM, Global R: 0.79, p-value = 0.001;
382 Fig. 7G). Nutrient addition shifted the composition of diazotrophs from gamma-, beta-, and
383 delta-proteobacteria toward several Cluster 1 gamma-proteobacterial *NifH* sequences (*NifH* OTU
384 608, 2012 and 95), sharing ≥ 89 % amino acid identity with *Pseudomonas stutzeri* (Moisander et
385 al. 2014, 2012), which comprised negligible proportions of initial EAC *NifH* sequences. Shifts in
386 the relative abundance of the three different gamma-proteobacterial *NifH* OTUs contributed to a
387 substantial proportion of the dissimilarity between diazotroph communities detected in EAC
388 nutrient treatments. For example, *NifH* OTU608 dominated NFe bottles, comprising up to 97 %
389 of *NifH* sequences and was responsible for 33 % of the average dissimilarity between t_0 and NFe
390 (SIMPER, 83 % total dissimilarity). In Si bottles, *NifH* OTU2012 represented up to 87 % of *NifH*
391 sequences detected, and contributed 41 % to the average dissimilarity between the t_0 and Si
392 bottles (SIMPER, 65 % dissimilarity). Similarly *NifH* OTU95 comprised up to 89 % of *NifH*
393 sequences in the Mix treatment and was responsible for 22% of the dissimilarity between the t_0
394 and diazotrophs in the Mix addition.

395 In contrast to *NifH* sequences retrieved from EAC nutrient treatments, the dominant *NifH* OTU
396 across CCE nutrient amendments was OTU2331, which shared 90 % amino acid identity to the
397 genus *Coralimargarita* of the Verrucomicrobia. In addition, sequences sharing 95 % *NifH*
398 amino acid identity with *Trichodemsium erythraeum* (OTU181) and *Candidatus*
399 *Atelocyanobacterium thalassa* (UCYN-A; OTU1321 and OTU50), were detected in the
400 unamended CCE diazotroph assemblages, but no such cyanobacterial *NifH* sequences were

401 present in the EAC. Differences in the relative abundance of these cyanobacterial diazotrophs
402 were observed between treatments, such as an increase in OTU181 from a maximum of 15 % in
403 the control to 62 % in the Si treatment, there were also significant shifts in diazotroph
404 composition between nutrient addition treatments (Fig. 7H) (ANOSIM, Global R: 0.69, p-value
405 = 0.004). Notably, there were no *NifH* sequences detected in the CCE Mix treatment.

406

407 **Time-dependent response to nutrient amendment: subcellular to community-level.** Daily
408 sampling of incubation bottles following nutrient amendment captured a cascade of effects at the
409 cellular, population and community level, indicating differences in the speed of response by
410 different microbes to nutrient resupply. Despite lower phytoplankton biomass, the EAC
411 community took up ~10 times more nitrate than the CCE community within the first 24 h (Fig.
412 8A and B). Net nitrate uptake in the EAC (averaged over day 1 to 3) was greatest in the Mix
413 ($2.98 \pm 0.88 \mu\text{M d}^{-1}$), and NFe and N treatments ($\sim 2 \mu\text{M d}^{-1}$), but was $< 0.3 \mu\text{M d}^{-1}$ in all other
414 treatments. In the CCE, the level of nitrate uptake was an order of magnitude lower, with rates
415 ranging from 0.02 to $0.25 \mu\text{M d}^{-1}$ (in the control and Mix, respectively). Net phosphate uptake by
416 both communities was relatively constant across nutrient amendments (~ 0.1 and $\sim 0.01 \mu\text{M d}^{-1}$ in
417 the EAC and CCE, respectively), with the exception of 30% higher rates in the EAC Mix
418 treatment (Fig. S3). Net silicate uptake rates in the EAC were greater than the CCE (~ 0.1 vs
419 $\sim 0.05 \mu\text{M d}^{-1}$, respectively), with rates increasing significantly (≥ 6 times) when Si was added
420 alone or with N, P and Fe (i.e., Mix treatment; Fig. S3). Total dissolved iron (TDFe)
421 concentrations at the end of the experiment were $0.38 \pm 0.07 \text{ nM}$ in the unamended EAC control
422 bottles, and $1.32 \pm 0.23 \text{ nM}$ in the CCE controls (Fig. S3), suggesting a strong Fe consumption
423 and thus a limited Fe potential contamination in the experiment (spikes were 10 nM).

424 To illustrate the impact of nutrient amendment at the cellular, population and community level in
425 the EAC and CCE, Fig. 8 shows time-dependent responses to the N treatment. The cellular
426 pigment content (as estimated using flow cytometer fluorescence emission detected at red/orange
427 wavelengths, corresponding to Chl-a/phycoerythrin) of EAC phototrophs in the N treatment was
428 relatively constant over the first 48 h, but then increased in both phycoerythrin-containing
429 prokaryotes and Chl-a-containing cells by t_{72} (Fig. 7C; Tables 2 and 3). In the CCE, N addition
430 caused rapid synthesis of Chl-a (but not phycoerythrin) in the first 24 h. By day 3 however,
431 phycoerythrin-containing prokaryotes in the CCE had doubled their pigment content, in a
432 manner that was similar to the observations in the EAC (Fig. 7D).

433 The initial ranked order abundance of microbial populations (as determined flow cytometrically)
434 was different in the EAC and CCE and showed variable temporal dynamics. N amendment of the
435 EAC community resulted in a doubling of total bacteria abundance within the first 24 h (Fig.
436 8E), but they then decreased to initial concentrations by t_{72} . The abundance of all but the large
437 picoeukaryote population declined in the EAC under N amendment, resulting in overall negative
438 phototrophic growth over the three day experiment ($-0.153 \pm 0.016 \text{ d}^{-1}$; Table S2). In contrast,
439 the abundance of all CCE phototroph populations increased within the first 24 h following N
440 amendment (Fig. 8D), and yielded significant positive growth during the experiment ($0.262 \pm$
441 0.043 d^{-1}).

442 Nutrient amendment caused a minor decline in the maximum quantum yield of PSII (F_V/F_M) in
443 the EAC microbial community with N addition (p-value = 0.013; Table 2), but had no effect on
444 F_V/F_M in the CCE community, remaining > 0.65 in the unamended controls (Fig. 8A). The light
445 saturating irradiance I_K was $\sim 50\%$ lower in the EAC, reflecting the greater depth of the sampled
446 community (Table 1), and despite lower phytoplankton biomass, carbon fixation rates in

447 unamended EAC bottles were higher than that of CCE controls (Fig. 8G and H). N amendment
448 of the EAC community lead to a significant increase in light utilisation efficiency (α) and light
449 saturated photosynthetic rate (P_{\max}) with no change in minimum saturating irradiance (I_K)
450 between the control and N enriched cells. There was however, a significant decline in I_K in the
451 NFe treatment (p-value < 0.05 Table 2). In the CCE, there was a significant increase in α and P_{\max}
452 with both N and NFe addition, with I_K lowest in the NFe treatment. There was a 1.7 times
453 increase in the maximum rate of primary productivity in the N amended treatment for the EAC
454 (p-value < 0.001), compared with a 2.7 times increase in the CCE (p-values < 0.001; Fig. 8G and
455 H). Co-addition of NFe resulted in a decrease in PP in the EAC (0.4 fold change), but a 6.28 fold
456 increase in PP in the CCE. This suggests stronger limitation of primary productivity in the CCE,
457 with a greater proportional increase in P_{\max} with NFe compared to N addition.

458

459 Discussion

460 The intensification of western boundary currents in the global ocean (Wu et al. 2012) raises
461 significant questions about their impact on microbial composition and biogeochemical activity,
462 particularly in light of the potential for WBCs to promote meso-scale eddy formation (Mata et al.
463 2007) and induce nutrient upwelling (Roughan & Middleton 2002). Here we show clear
464 differences in the vertical nutrient structure of a cyclonic cold-core eddy relative to adjacent
465 waters, and an increase in microbial diversity and size structure of an eddy assemblage relative to
466 an adjacent western boundary current, the EAC. Our results indicate that cyclonic eddies
467 increase delivery of N to the upper ocean but also increase the biological demand for Fe that is

468 necessary to sustain the growth of large-celled phototrophs and potentially support the diversity
469 of diazotrophs over longer time-scales.

470 **Responses of microbes to nutrient amendment.**

471 Previous studies in the Tasman Sea region have determined that surface phytoplankton
472 communities are limited by N (Hassler et al. 2011; Hassler et al. 2014; Ellwood et al. 2013), and
473 that diazotrophs (cyanobacteria that are able to bypass nitrate limitation by fixing atmospheric N)
474 inhabit waters to ~100 m following nutrient draw-down over the summer (Moisander et al.
475 2010). Our observations show that EAC phytoplankton sampled at 80 m below the surface are
476 also N limited, and that upwards displacement of isopycnal surfaces induced by a cyclonic eddy
477 introduces nutrients into the euphotic zone to alleviate potential N limitation (Fig. 4).
478 Phytoplankton in the CCE (sampled at ~40 m) were also limited by N, but rates of carbon
479 fixation more than doubled under NFe relative to N amendment, likely due to the different
480 species composition underpinning primary productivity. In both water masses, a positive
481 response in Chl-a was also seen with addition of N+Fe+Si+P, suggesting co-limitation by
482 multiple nutrients in both water masses, likely a result of different nutrient requirements by
483 different phototrophs. Uplift of N together with Fe and other nutrients would therefore increase
484 the rate of biomass production in the eddy as well as increase the relative abundance of diatoms,
485 both of which could act to increase export production relative to adjacent waters.

486 While the starting communities in the EAC and CCE were distinct, microbial phototrophs
487 showed similar responses to nutrient amendment in both water masses, with NFe addition to the
488 EAC resulting in phototrophs more similar to those in the initial CCE community (Fig. 7C).
489 Fucoxanthin containing cells (likely diatoms that contribute significantly to export production;

490 Honjo et al. 1995) became more prevalent in NFe and Mix treatments, whereas haptophytes
491 clearly diminished under these amendments. Similarly, peridinin-containing dinoflagellates were
492 initially present in both communities, but their abundance declined with nutrient amendment,
493 becoming undetectable amongst other EAC microbes at the end of our experiment.
494 *Prochlorococcus* was an order of magnitude more abundant in the EAC relative to the CCE,
495 consistent with the warmer “tropical” signature of this western boundary current (Seymour et al.
496 2012), and declined in abundance in the Mix treatment. In the CCE samples, *Prochlorococcus*
497 similarly decreased in the Si and Mix treatments. *Synechococcus* had a positive response to
498 bottle enclosure but unlike other studies (Moisander et al. 2012), we found that its abundance
499 was similar in control and enriched treatments. Maximum net growth rates were observed in the
500 eddy NFe bottles for *Prochlorococcus* ($0.345 \pm 0.047 \text{ d}^{-1}$), small picoeukaryotes (0.212 ± 0.033
501 d^{-1}) and large picoeukaryotes (i.e., nano-eukaryotes; $0.297 \pm 0.059 \text{ d}^{-1}$), but for *Synechococcus*,
502 maximum growth was found in CCE controls ($0.324 \pm 0.047 \text{ d}^{-1}$, relative to $0.194 \pm 0.035 \text{ d}^{-1}$
503 with NFe amendment).

504 Among the heterotrophic bacteria, initial EAC and CCE populations displayed similar abundance
505 and alpha-diversity, and nutrient amendment lead to compositional shifts in both water masses.
506 Addition of nitrate to the EAC community caused a doubling of total bacteria abundance within
507 the first 24 h. Bacteria also became more abundant in the CCE community after 3 days within the
508 Si and Mix bottles. Elevated bacteria abundance is likely to have arisen through increased
509 dissolved organic matter (DOM) production by the resident community via several potential
510 mechanisms: (1) mortality and cell lysis; (2) elevated rates of DOM release due to nutrient
511 supplementation; and (3) altered microbial composition. While we did not measure rates of

512 DOM production, our data certainly demonstrate coupling between autotrophs and heterotrophs,
513 just as in a previous study (Baltar et al. 2010).

514 **Diazotroph relative abundance and diversity.** Across the global ocean, the main supply of
515 nitrogen into surface waters is via transport from below the thermocline, but in many regions
516 significant amounts of new nitrogen may also be supplied via nitrogen fixation (Capone et al.
517 2005; La Roche & Breitbart 2005). Our molecular analyses revealed the presence of
518 heterotrophic gamma-proteobacterial diazotrophs in the sub-surface EAC microbial community,
519 whereas cyanobacterial diazotrophs (i.e., *Trichodesmium* and UCYN-A) were detected in the
520 CCE. Given the relatively high iron requirement of diazotrophs (Kustka et al., 2003), as well as
521 their low reliance on dissolved inorganic N, we expected to see a divergent response of the
522 diazotrophs to nutrient amendment. Indeed, in the Mix bottles, diazotrophs became undetectable
523 in the CCE samples, and were clearly outcompeted by the eukaryote phototrophs. Nutrient
524 addition resulted in *NifH* OTU2331 becoming more prominent across CCE nutrient amendments.
525 This OTU shares 90 % amino acid identity to the genus *Coralimargarita* of the
526 Verrucomicrobia, and was not present amongst the EAC diazotrophs. In the EAC, nutrient
527 addition caused a shift from the mixed proteobacterial community observed at t0, to *NifH*
528 OTU608, *NifH* OTU2012 and *NifH* OTU95. These OTUs represent distinct taxa at the 95%
529 sequence similarity level, yet share the same % identity at the amino acid level, falling within the
530 same clade of Cluster 1 gamma-proteobacterial diazotrophs. The physiology or genome content
531 of these taxa remains completely unknown, but they seem to be abundant in warm, oligotrophic
532 surface waters globally (Langlois et al., 2005). In the southwestern Pacific, the abundance of this
533 group has been shown to be correlated to DOC concentration, and to increase with Fe and P
534 addition (Moisander et al., 2012). In contrast, the dominant diazotroph in the CCE was an OTU

535 sharing 95 % *NifH* amino acid identity with *Trichodemsium erythraeum* (OTU181) and OTUs
536 matching *Candidatus Atelocyanobacterium thalassa* (UCYN-A; OTU1321 and OTU50).
537 UCYN-A is the dominant diazotroph in the Coral Sea (source of the EAC) during the austral
538 spring (Messer et al., 2015), and is also relatively abundant in the western South Pacific
539 (Moisander et al., 2010). UCYN-A abundance has previously been shown to increase in response
540 to Fe and organic carbon additions (Moisander et al., 2012), while Fe has also been shown to
541 increase the rate of N₂ fixation by UCYN-A (Krupke et al., 2015).

542 Our observations demonstrate the presence of heterotrophic N₂-fixing organisms in sub-surface
543 waters with strong nitrate deficiency (but not necessarily low nitrate concentration; Fig. 2);
544 however, a remaining research need is to conduct N₂-fixation rate measurements in conjunction
545 with diazotroph diversity assessment to verify whether this process represents a significant
546 source of new N within and outside eddies, and whether changes in N₂-fixation are due to a shift
547 in diversity or a change in *NifH* expression.

548 **Physiological responses to nutrient supply.** At the cellular level, N addition caused rapid
549 pigment synthesis (doubling of normalised fluorescence per cell) in the CCE assemblage within
550 the first 24 h after amendment, indicating that nutrient uplift could initially cause ‘greening’ in
551 the absence of an increase in cellular biomass (Behrenfeld et al. 2015). By the end of our
552 experiments, both phycoerythrin and Chl-a quotas increased in both water masses with N
553 amendment, concomitant with an increase in total Chl-a, suggesting both pigment synthesis and
554 biomass production contributed to elevated Chl-a. These observations are of obvious importance
555 for the accurate interpretation of satellite and other in situ Chl-a fluorescence data within meso-
556 scale eddy features.

557 Photophysiological changes such as a decline in PSII turnover time, cross-sectional area and
558 increased electron transport rates have been detected upon relief of nutrient limitation (Milligan,
559 Aparicio & Behrenfeld 2012). We detected minimal change in the photochemical efficiency
560 (maximum quantum yield of PSII) with nutrient amendment, but there were measureable
561 changes in the shape of the photosynthesis-irradiance (P-I) curve. Nitrate amendment of the EAC
562 community increased light utilisation efficiency and light saturated photosynthetic rates,
563 indicating increased photosynthetic electron transport and antenna size. Our flow cytometry data
564 suggest that this was likely due to increased chlorophyll quota rather than an increase in cross
565 sectional area (Fig. 7D). In the CCE community, the greatest change in carbon fixation (P-I)
566 parameters was measured in the NFe treatment, suggesting an increase in PSII units per cell
567 (detected via increased pigment quotas after 24 h), as well as an increase in total photosynthetic
568 biomass, resulting in increased electron transport rates and light capturing capacity.

569 **Nutrient uptake dynamics.** Initial uptake rates of nitrate (i.e. within the first day) by the EAC
570 community were 10 times higher than in the CCE despite 3-fold lower phytoplankton biomass.
571 This is consistent with the opportunistic nutrient uptake strategies of phytoplankton in
572 oligotrophic habitats (McCarthy & Goldman 1979) and the theory that fast growing algae (with
573 small cell size) are stimulated by short-term nutrient supply (Pederson & Borum 1996).
574 However, it is unlikely that such high nutrient uptake rates would be sustained in the EAC,
575 largely because nutrient inputs (of the magnitude used in our experiments) are episodic and often
576 coincide with major physical disturbances such as cyclones (e.g. Law et al. 2011). A comparison
577 of the initial EAC and CCE communities suggests that prolonged nutrient inputs within cyclonic
578 eddies results in a shift toward larger cells which generally have greater capacity for nutrient
579 storage and higher nutrient requirements for growth (Litchman et al. 2007).

580 Despite these potential experimental artefacts, the relative differences in nutrient demand
581 between treatments show that maximum net uptake rates in both water masses occurred when all
582 macronutrients were added together, compared to treatments which contained a surplus of N, P
583 or Si relative to other macronutrients and iron. Under N amendment, uptake ratios of N:P in the
584 EAC were ~20 compared to ~10 in the CCE, and uptake ratios of N:Si were ~10 and 4 in the
585 EAC and CCE, respectively, but they were closer to Redfield (Si:N:Pi = 1:1:16) in the Mix
586 treatment (Fig. S2). This indicates that the vertical distribution of nutrients relative to one
587 another will regulate microbial responses to eddy-induced uplift, as has been shown by Bibby
588 and Moore (2011) with respect to N:Si in the sub-tropical north Atlantic and central Pacific near
589 Hawai'i.

590 **Conclusions**

591 Phytoplankton community structure plays an important role in the ecology and biogeochemistry
592 of pelagic ecosystems including the export of organic matter to the deep ocean and the
593 sequestration of carbon (Follows & Dutkiewicz 2011; Karl et al. 2012). Here we show that
594 cyclonic eddies enhance primary production in this WBC region by delivering nitrate to the
595 upper ocean. The enhanced productivity was driven largely by an increase in the abundance of
596 diatoms, with a concomitant decline in the abundance of haptophytes and peridinin-containing
597 dinoflagellates.

598 This study confirms the low-nutrient low Chl-a status of the Eastern Australian Current (EAC) to
599 sub-surface depths of ~80 m, and provides the first evidence of N and Fe co-limitation in an
600 adjacent cyclonic eddy, demonstrating that such meso-scale features have the potential to
601 increase internal nutrient inputs into the upper ocean and thereby change microbial composition

602 and nutrient demand. Importantly, eddies may provide a critical compensatory mechanism to
603 enrich the upper ocean and counteract increasing stratification occurring under climate change
604 (Matear et al. 2013). The divergent response of large phototrophs and diazotrophs in our nutrient
605 amendment experiments suggests that N₂-fixing cyanobacteria and heterotrophic bacteria are an
606 important functional group to include in biogeochemical models, whose abundance and diversity
607 have been under-appreciated in this region until recently (Messer et al., 2015).

608

609 **Acknowledgements.**

610 We thank the officers and crew of the *R/V Southern Surveyor* and the Bio-optics voyage
611 participants, particularly Massimo Pernice (Instituto de Ciencias del Mar- Consejo Superior de
612 Investigacion Cientifica, Spain) for assistance with sampling, Andrew Bowie for dissolved Fe
613 flow injection analyses, as well as Jennifer Clark (University of Technology Sydney) for flow
614 cytometry analyses.

615

616

617 **References**

618 Acosta Martinez V, Dowd SE, Sun Y, Allen V (2008) Tag-encoded pyrosequencing analysis of
619 bacterial diversity in a single soil type as affected by management and land use. *Soil Biology and*
620 *Biochemistry*. 40(11):2762-2770.

621 Altschul S, Gish W, Miller W, Myers E, Lipman D (1990) Basic local alignment search tool.
622 *Journal of Molecular Biology* **215**:403–410.
623 <http://www.sciencedirect.com/science/article/pii/S0022283605803602> (Accessed December 13,
624 2013).

625 Baltar F, Ari´stegui J, Gasol JM, Lekunberri I, Herndl GJ (2010) Mesoscale eddies: hotspots of
626 prokaryotic activity and differential community structure in the ocean. *The ISME Journal* **4**:
627 975–988.

628 Barlow RG, Stuart V, Lutz V, Sessions H, Sathyendranath S, Platt T, Kyewalyanga M,
629 Clementson L, Fukasawa M, Watanage S, Devred E (2007) Seasonal pigment patterns of surface
630 phytoplankton in the subtropical southern hemisphere. *Deep-Sea Research I* **54**:1687-1703.

631 Behrenfeld M (2011) Biology: Uncertain future for ocean algae. *Nature Climate Change* **1**:33–34
632 doi:10.1038/nclimate1069.

- 633 Behrenfeld MJ, O'Malley RT, Boss ES, Westberry TK, Graff JR, Halsey KH, Milligan AJ,
634 Siegel DA and Brown TB (2015) Revaluating ocean warming impacts on global phytoplankton.
635 Nature Climate Change doi: 10.1038/NCLIMATE2838.
- 636 Bibby TS, Gorbunov MY, Wyman KW, Falkowski PG (2008) Photosynthetic community
637 responses to upwelling in mesoscale eddies in the subtropical North Atlantic and Pacific Oceans.
638 Deep-Sea Research II **55**: 1310-1320.
- 639 Bibby TS, Moore CM (2011) Silicate:nitrate ratios of upwelled waters control the phytoplankton
640 community sustained by mesoscale eddies in sub-tropical North Atlantic and Pacific.
641 Biogeosciences **8**: 657–666.
- 642 Brzezinski MA, Nelson DM (1989). Seasonal changes in the silicon cycle within a Gulf Stream
643 warm-core ring. Deep-Sea Research 36: 1009-1023.
- 644 Capone DG, Burns JA, Montoya JP, Subramaniam A, Mahaffey C, Gunderson T, Michaels AF,
645 Carpenter EJ. (2005) Nitrogen fixation by *Trichodesmium* spp.: An important source of new
646 nitrogen to the tropical and subtropical North Atlantic Ocean. Global Biogeochemical Cycles
647 19(2) GB2024
- 648 Caporaso J, Kuczynski J, Stombaugh J, Bittinger K, Bushman F, Costello EK, et al. (2010).
649 QIIME allows analysis of high-throughput community sequencing data. Nature Methods 7:335–
650 336. <http://dx.doi.org/10.1038/nmeth0510-335> (Accessed December 7, 2013).
- 651 Chelton DB, Schlax MG, Samelson RM (2011) Global observations of nonlinear mesoscale
652 eddies. Progress in Oceanography **91**:167–216.
- 653 Clarke K (1993). Non-parametric multivariate analyses of changes in community structure.
654 Australian Journal of Ecology **18**:117–143. <http://onlinelibrary.wiley.com/doi/10.1111/j.1442-9993.1993.tb00438.x/full> (Accessed January 13, 2014).
- 656 Clarke K, Warwick R (2001) Change in marine communities: an approach to statistical analysis
657 and interpretation 2nd Edition. PRIMER-E Ltd: Plymouth
658 <http://www.opengrey.eu/item/display/10068/595716> (Accessed January 14, 2014).
- 659 Cowley R, Critchley G, Eriksen R, Latham V, Plaschke R, Rayner M, Terhell D (1999) CSIRO
660 Marine Laboratories Report 236 Hydrochemistry Operations Manual. Technical report, CSIRO
661 Marine Laboratories, Hobart, Australia.
- 662 Deutsch C, Weber T (2012) Nutrient Ratios as a Tracer and Driver of Ocean Biogeochemistry
663 Annual Review of Marine Science **4**:113–41.
- 664 Doblin MA, Ralph PJ, Petrou KL, Shelly K, Westwood K, van den Enden R, Wright S, Griffiths
665 B (2011) Diel variation of chl-a fluorescence, phytoplankton pigments and productivity in the
666 Sub-Antarctic Zone. Deep Sea Research II: Topical studies in oceanography **58**:2189-2199.
- 667 Dowd SE, Callaway TR, Wolcott RD, Sun Y, McKeehan T, Hagevoort RG, et al. (2008)
668 Evaluation of the bacterial diversity in the feces of cattle using 16S rDNA bacterial tag-encoded

- 669 FLX amplicon pyrosequencing (bTEFAP). *BMC Microbiology* **8**:125.
670 <http://www.pubmedcentral.nih.gov/articlerender.fcgi?artid=2515157&tool=pmcentrez&renderty>
671 [pe=abstract](http://www.pubmedcentral.nih.gov/articlerender.fcgi?artid=2515157&tool=pmcentrez&renderty) (Accessed January 23, 2014).
- 672 Edgar RC (2010) Search and clustering orders of magnitude faster than BLAST. *Bioinformatics*
673 **26**:2460–2461. <http://www.ncbi.nlm.nih.gov/pubmed/20709691> (Accessed November 7, 2013).
- 674 Ellwood MJ, Law CS, Hall, J., Boyd PW (2013) Relationships between nutrient stocks and
675 inventories and phytoplankton physiological status along an oligotrophic meridional transect in
676 the Tasman Sea. *Deep-Sea Research I* **72**:102-120.
- 677 Everett JD, Baird ME, Oke PR, Suthers IM (2012) An Avenue of Eddies: Quantifying the
678 biophysical properties of mesoscale eddies in the Tasman Sea. *Geophysical Research Letters* **39**:
679 L16608 doi:10.1029/2012GL053091.
- 680 Everett JD, Baird ME, Roughan M, Suthers IM, Doblin MA (2014) Relative impact of seasonal
681 and oceanographic drivers of surface chlorophyll-a along a western boundary current. *Progress*
682 *in Oceanography* **120**:340-351.
- 683 Farnelid H, Andersson AF, Bertilsson S, Al-Soud WA, Hansen LH, Sørensen S, et al. (2011)
684 Nitrogenase gene amplicons from global marine surface waters are dominated by genes of non-
685 cyanobacteria. *PLoS One* **6**:e19223.
686 <http://www.pubmedcentral.nih.gov/articlerender.fcgi?artid=3084785&tool=pmcentrez&renderty>
687 [pe=abstract](http://www.pubmedcentral.nih.gov/articlerender.fcgi?artid=3084785&tool=pmcentrez&renderty) (Accessed March 14, 2013).
- 688 Farnelid H, Bentzon-Tilia M, Andersson AF, Bertilsson S, Jost G, Labrenz M, et al. (2013).
689 Active nitrogen-fixing heterotrophic bacteria at and below the chemocline of the central Baltic
690 Sea. *The ISME Journal* **7**:1413–1423.
- 691 Fish JA, Chai B, Wang Q, Sun Y, Brown CT, Tiedje JM, et al. (2013) FunGene: the functional
692 gene pipeline and repository. *Frontiers of Microbiology* **4**:291.
693 <http://www.pubmedcentral.nih.gov/articlerender.fcgi?artid=3787254&tool=pmcentrez&renderty>
694 [pe=abstract](http://www.pubmedcentral.nih.gov/articlerender.fcgi?artid=3787254&tool=pmcentrez&renderty) (Accessed February 5, 2014).
- 695 Foldager Pedersen M, Borum J (1996) Nutrient control of algal growth in estuarine waters.
696 Nutrient limitation and the importance of nitrogen requirements and nitrogen storage among
697 phytoplankton and species of macroalgae. *Marine Ecology Progress Series* **142**:261-272.
- 698 Follows MJ, Dutkiewicz S, Grant S, Chisholm SW (2007) Emergent biogeography of microbial
699 communities in a model ocean. *Science* **315**:1843–1846.
- 700 Follows MJ, Dutkiewicz S (2011) Modeling Diverse Communities of Marine Microbes. *Annual*
701 *Review of Marine Science* **3**:427–451.
- 702 Gasol JM, Del Giorgio PA (2000) Using flow cytometry for counting natural planktonic bacteria
703 and understanding the structure of planktonic bacterial communities. *Scientifica Marina* **64**:
704 197–224

- 705 Gaube P, McGillicuddy DJ Jr, Chelton DB, Behrenfeld MJ, Strutton PG (2014) Regional
706 variations in the influence of mesoscale eddies on near-surface chlorophyll. *Journal of*
707 *Geophysical Research Oceans* **119**:8195–8220.
- 708 Hagino K, Onuma R, Kawachi M, Horiguchi T (2013) Discovery of an Endosymbiotic Nitrogen-
709 Fixing Cyanobacterium UCYN-A in *Braarudosphaera bigelowii* (Prymnesiophyceae). *PLoS*
710 *ONE* **8**: e81749. doi:10.1371/journal.pone.0081749
- 711 Hassler C, Djajadikarta RJ, Doblin MA, Everett JD, Thompson P (2011) Characterisation of
712 water masses and nutrient limitation of phytoplankton in the separation zone of the East
713 Australian Current in spring 2008. *Deep Sea Research II, special issue on East Australian*
714 *Current*. **58**:664-677.
- 715 Hassler CS, Ridgway K, Bowie AR, Butler ECV, Clementson L, Doblin MA, Ralph P, Law CS,
716 Davies DM, van der Merwe P, Watson R, Ellwood, MJ (2014) Primary productivity induced by
717 Iron and Nitrogen in the Tasman Sea-An overview of the PINTS expedition. *Marine and*
718 *Freshwater Research* **65**:517-537.
- 719 Honjo S, Dymond J, Collier R, Manganini SJ (1995) Export production of particles to the
720 interior of the equatorial Pacific Ocean during the 1992 EqPac experiment. *Deep Sea Research II*
721 **42**:831-870.
- 722 Hood RR, Laws EA, Armstrong RA, Bates NR, Brown CW, Carlson CA, Chai F, Doney SC,
723 Falkowski PG, Feely RA, Friedrichs MAM, Landry MR, Moore KJ, Nelson DM, Richardson
724 TL, Salihoglu B, Schartau M, Toole DA, Wiggert JD (2006) Pelagic functional group modeling:
725 Progress, challenges and prospects. *Deep-Sea Research Part II-Topical Studies in Oceanography*
726 **53**:459-512.
- 727 Karl DM, Church MJ, Doreb JE, Letelier RM and Mahaffey C (2012) Predictable and efficient
728 carbon sequestration in the North Pacific Ocean supported by symbiotic nitrogen fixation.
729 *Proceedings National Academy Science* **109**:1842–1849.
- 730 Kustka AS, Sañudo-Wilhelmy S, Carpenter EJ, Capone DG, Raven, JA (2003) A revised
731 estimate of the iron efficiency of nitrogen fixation with special reference to the marine
732 cyanobacterium *Trichodesmium* spp. (cyanophyta). *Journal of Phycology* **39**:12–25.
- 733 Krupke A, Mohr W, LaRoche J, Fuchs BM, Amann RI, Kuypers MM (2015) The effect of
734 nutrients on carbon and nitrogen fixation by the UCYN-A-haptophyte symbiosis. *ISME*
735 *J.* **9**:1635-47. La Roche J, Breitbarth E (2005) Importance of diazotrophs as a source of new
736 nitrogen in the ocean. *Journal of Sea Research* **53**:67-69.
- 737 Langlois RJ, LaRoche J, Raab PA (2005) Diazotrophic Diversity and Distribution in the Tropical
738 and Subtropical Atlantic Ocean. *Applied and Environmental Microbiology* **71**:7910–7919.
- 739 Law CS, Woodward EMS, Ellwood MJ, Marriner A, Bury SJ, Safi KA (2011) Response of
740 surface nutrient inventories and nitrogen fixation to a tropical cyclone in the southwest Pacific.
741 *Limnology and Oceanography* **56**:1372–1385.

- 742
743 Liu H, Probert I, Uitz J, Claustre H, Aris-Brosou S, Frada M, Not F, de Vargas C (2009)
744 Extreme diversity in noncalcifying haptophytes explains a major pigment paradox in open
745 oceans. *Proceedings of the National Academy of Science* **106**:12803–12808.
746
- 747 Litchman E, Klausmeier CA, Schofield OM, Falkowski PG (2007) The role of functional traits
748 and trade-offs in structuring phytoplankton communities: scaling from cellular to ecosystem
749 level. *Ecology Letters* **10**:1170–1181.
- 750 Marie D, Partensky F, Jacquet S, Vaulot D (1997) Enumeration and cell cycle analysis of natural
751 populations of marine picoplankton by flow cytometry using the nucleic acid stain SYBR Green
752 I. *Applied Environmental Microbiology* **63**:186–193.
- 753 Martin JH, Gordon RM and Fitzwater SE (1991) The case for iron. *Limnology and Oceanography*
754 **36**:1793-1802.
- 755 Mata MM, Wijffels S, Tomczak M, Church JA (2007) Eddy shedding and energy conversions in
756 the East Australian Current. *Journal of Geophysical Research* **111**: C09034,
757 doi10.1029/2006JC003592.
- 758 Matear RJ, Chamberlain MA, Sun C, Feng M (2013) Climate change projection of the Tasman
759 Sea from an Eddy-resolving Ocean Model. *Journal of Geophysical Research Oceans* **118**: 2961–
760 2976.
- 761 McCarthy JJ, Goldman JC (1979) Nitrogenous nutrition of marine phytoplankton in nutrient-
762 depleted waters. *Science* **203**:670-672.
- 763 McGillicuddy DJ Jr (2016) Mechanisms of physical-biological-biogeochemical interaction at the
764 oceanic mesoscale. *Annual Review of Marine Science* **8**:13.1–13.36.
- 765 McGillicuddy DJ Jr, Robinson AR, Siegel DA, Jannasch HW, Johnson R, et al. (1998) Influence
766 of mesoscale eddies on new production in the Sargasso Sea. *Nature* **394**:263–265.
- 767 Messer LF, Mahaffey C, Robinson C, Jeffries TC, Baker KG, Bibiloni Isaksson J, Ostrowski M,
768 Doblin MA, Brown MV, Seymour JR (2015) High levels of heterogeneity in diazotroph diversity
769 and activity within a putative hotspot for marine nitrogen fixation. *The ISME Journal*,
770 doi:10.1038/ismej.2015.205.
- 771 Milligan AJ, Aparicio UA, Behrenfeld MJ (2012) Fluorescence and nonphotochemical
772 quenching responses to simulated vertical mixing in the marine diatom *Thalassiosira weissflogii*.
773 *Marine Ecology Progress Series* **448**:67-78.
- 774 Moisander PH, Serros T, Paerl RW, Beinart R, Zehr JP (2014) Gammaproteobacterial
775 diazotrophs and nifH gene expression in surface waters of the South Pacific Ocean. *The ISME*
776 *Journal* **8**:1962-1973.
- 777 Moisander PH, Zhang R, Boyle E, Hewson I, Montoya JP, Zehr JP (2012) Analogous nutrient
778 limitations in unicellular diazotrophs and *Prochlorococcus* in the South Pacific Ocean. *The*
779 *ISME Journal* **6**:733–44.

- 780 Moisaner PH, Beinart RA, Hewson I, White AE, Johnson KS, Carlson CA, Montoya JP, Zehr
781 JP (2010) Unicellular cyanobacterial distributions broaden the oceanic N₂ fixation domain.
782 *Science* **327**:1512-1514.
- 783 Nelson DM, McCarthy JJ, Joyce TM, Ducklow HW (1989) Enhanced near-surface nutrient
784 availability and new production resulting from the frictional decay of a Gulf Stream warm-core
785 ring. *Deep-Sea Research A* **36**:705–714.
- 786 Moore CM, Mills MM, Arrigo KR, Berman-Frank I, Bopp L, Boyd PW, Galbraith ED, Geider
787 RJ, Guieu C, Jaccard SL, Jickells RJ, La Roche J et al. (2013) Processes and patterns of oceanic
788 nutrient limitation. *Nature Geoscience* **6**:701-710.
- 789 Platt T, Gallegos CL, Harrison WG (1980) Photoinhibition of photosynthesis in natural
790 assemblages of marine phytoplankton. *Journal of Marine Research* **38**:687-701.
- 791 Quast C, Pruesse E, Yilmaz P, Gerken J, Schweer T, Yarza P, et al. (2013) The SILVA
792 ribosomal RNA gene database project: improved data processing and web-based tools. *Nucleic
793 Acids Research* **41**:D590–6.
794 [http://www.pubmedcentral.nih.gov/articlerender.fcgi?artid=3531112&tool=pmcentrez&renderty
795 pe=abstract](http://www.pubmedcentral.nih.gov/articlerender.fcgi?artid=3531112&tool=pmcentrez&rendertype=abstract) (Accessed November 8, 2013).
- 796 Ridame C, Le Moal M, Guieu C, Ternon E, Biegala IC, L'Helguen S, et al. (2011) Nutrient
797 control of N₂ fixation in the oligotrophic Mediterranean Sea and the impact of Saharan dust
798 events. *Biogeosciences* **8**:2773–2783. <http://www.biogeosciences.net/8/2773/2011/> (Accessed
799 March 6, 2014).
- 800 Ridgway K, Godfrey J (1997) Seasonal cycle of the East Australian Current. *Journal of
801 Geophysical Research* **102**:22,921–22,936.
- 802 Roughan M, Middleton J (2002) A comparison of observed upwelling mechanisms off the east
803 coast of Australia. *Continental Shelf Research* **22**:2551–2572.
- 804 Schreiber U (2004) Pulse-Amplitude-Modulation (PAM) fluorometry and saturation pulse
805 method: an overview. In: Papageorgiou G, Govindjee (eds) *Chlorophyll a fluorescence: a
806 signature of photosynthesis*. Springer. Dordrecht pp 279-319.
- 807 Seymour JR, Seuront L, Mitchell JG (2007) Microscale gradients of planktonic microbial
808 communities above the sediment surface in a mangrove estuary. *Estuarine, Coastal and Shelf
809 Science* **73**:651-666.
- 810 Seymour JR, Doblin MA, Jeffries TC, Brown MV, Newton K, Ralph PJ, Baird M, Mitchell JG
811 (2012) Contrasting microbial assemblages in adjacent water-masses associated with the East
812 Australian Current. *Environmental Microbiology Reports* **4**:548-555.
- 813 Turk-Kubo KA, Achilles KM, Serros TRC, Ochiai M, Montoya JP, Zehr JP (2012) Nitrogenase
814 (nifH) gene expression in diazotrophic cyanobacteria in the Tropical North Atlantic in response
815 to nutrient amendments. *Frontiers of Microbiology* **3**:386-403.

- 816 [http://www.pubmedcentral.nih.gov/articlerender.fcgi?artid=3487379&tool=pmcentrez&renderty](http://www.pubmedcentral.nih.gov/articlerender.fcgi?artid=3487379&tool=pmcentrez&rendertype=abstract)
817 [pe=abstract](http://www.pubmedcentral.nih.gov/articlerender.fcgi?artid=3487379&tool=pmcentrez&rendertype=abstract) (Accessed November 12, 2012).
- 818 Uitz J, Huot Y, Bruyant G, Babin M, Claustre H (2008) Relating phytoplankton
819 photophysiological properties to community structure on large scales. *Limnology and*
820 *Oceanography* **53**:614-630.
- 821 Waite AM, Pesant S, Griffin DA, Thompson PA, Holl CM (2007) *Oceanography*, primary
822 production and dissolved inorganic nitrogen uptake in two Leeuwin Current eddies. *Deep-Sea*
823 *Research II* **54**:981–1002.
- 824 Wang Q, Quensen J, Fish J, Lee T, Sun Y, Tiedje J, et al. (2013) Ecological patterns of nifH
825 genes in four terrestrial climatic zones explored with targeted metagenomics using FrameBot, a
826 new informatics tool. *MBio* 4:e00592–13. <http://mbio.asm.org/content/4/5/e00592-13.short>
827 (Accessed March 6, 2014).
- 828 Wu L, Cai W, Zhang L, Nakamura H, Timmermann A, Joyce T, McPhaden MJ, Alexander M,
829 Qiu B, Visbeck M, Chang P, Giese B (2012) Enhanced warming over the global subtropical
830 western boundary currents. *Nature Climate Change* **2**:161–166.
- 831 Zehr J, Jenkins B, Short S, Steward G (2003) Nitrogenase gene diversity and microbial
832 community structure: a cross system comparison. *Environmental Microbiology* **5**:539–554.
833 <http://onlinelibrary.wiley.com/doi/10.1046/j.1462-2920.2003.00451.x/full> (Accessed April 5,
834 2013).
- 835 Zehr J, McReynolds L (1989) Use of degenerate oligonucleotides for amplification of the nifH
836 gene from the marine cyanobacterium *Trichodesmium thiebautii*. *Applied Environmental*
837 *Microbiology* **55**:2522–2526.
- 838 Zehr J, Turner P (2001) Nitrogen fixation: Nitrogenase genes and gene expression. *Methods*
839 *Microbiology* **30**:271–285.
- 840 Zehr JP, Mellon MT, Hiorns WD (1997) Phylogeny of cyanobacterial nifH genes: evolutionary
841 implications and potential applications to natural assemblages. *Microbiology* **143**:1443–1450.

843 **Tables**

844 Table 1: Starting conditions for nutrient amendment experiments in the East Australian Current
 845 (EAC) and a cyclonic cold core eddy (CCE). Note that sampling depths targeted the chlorophyll-
 846 a fluorescence maximum (Fmax), which was deeper in the EAC than the CCE.

	EAC	CCE
Location	29.14817 °S, 154.31495 °E	32.35217 °S, 153.58112 °E
Bottom depth (m)	3279	4632
Sampling depth (Fmax, m)	80	41
Temperature (°C)	21.08	21.31
Salinity	35.52	35.49
Ammonium (μM)	0.07 ± 0.02	0.16 ± 0.01*
Nitrate (μM)	0.26 ± 0.24	0.14 ± 0.02
Phosphate (μM)	0.12 ± 0.02	0.11 ± 0.01
Silicate (μM)	0.84 ± 0.03	0.52 ± 0.01
Total dissolved iron (TDFe) in controls at t72 (nM)	0.38 ± 0.07	1.32 ± 0.23
Chlorophyll-a (μg L ⁻¹)	0.106 ± 0.008	0.336 ± 0.041

847 *analytical replicates from same CTD cast, not separate casts as for EAC (n = 2)

848

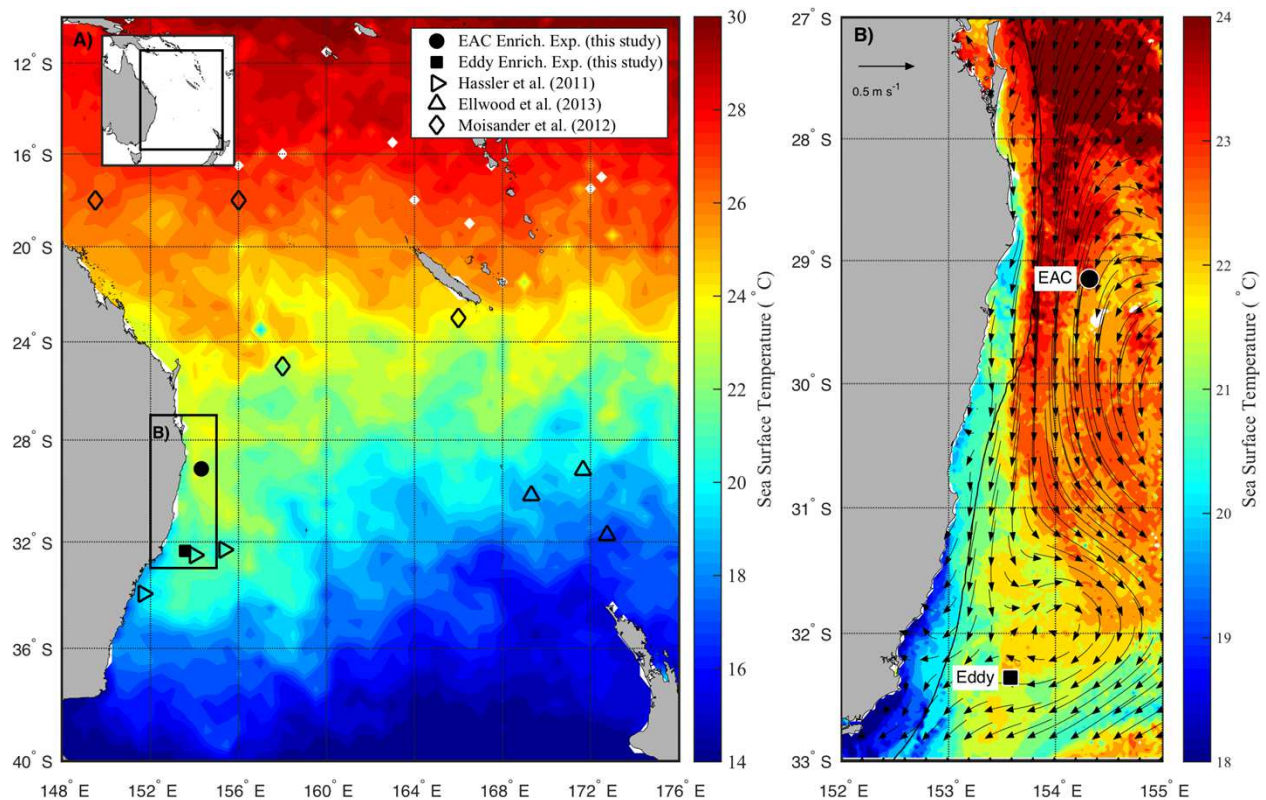
850 Table 2: Effect of experimental manipulation on microbial assemblages in the East Australian
 851 Current (EAC) and a cyclonic cold core eddy (CCE) as shown by comparison of t_0 with t_{72} no
 852 amendment control, as well as t_{72} nutrient amendments relative to controls. Treatments include
 853 NO_3 (10 μM nitrate final concentration), NO_3+Fe (10 μM nitrate and 1 nM Fe final
 854 concentration), Si (10 μM final concentration), and Mix (N+Si+P+Fe; 10N : 10Si : 0.625P μM in
 855 Redfield proportions and 1 nM Fe respectively). ++ strong positive difference, $P<0.01$; +
 856 positive difference, $P<0.05$; --strong negative difference, $P<0.01$; - negative difference, $P<0.05$;
 857 blank cells: no significant difference; nd: not detected; shaded cells: no measurement.
 858
 859

Parameter	Comparison of t_0 versus t_{72} control		Comparison of t_{72} nutrient amendments versus t_{72} control							
			NO_3		NO_3+Fe		Si		Mix	
	EAC	CCE	EAC	CCE	EAC	CCE	EAC	CCE	EAC	CCE
Chlorophyll a		-	+	+	+	+			+	+
Fucoxanthin:Chl a				+	+	+			+	+
Hex-Fuco:Chl a	-				-	-				
Peridinin:chl a	nd		nd	-	nd	-	nd	-		
Cell abundance*										
- Total pico and nano eukaryote	--	+							--	
- <i>Prochlorococcus</i>	--							--		
- <i>Synechococcus</i>	+	+							--	--
- Picoeukaryote			--					--	--	
- Nanoeukaryote						+				
- Bacteria								++		++
F_V/F_M			-							
Chl-a fluorescence/cell	--		++	++	++	--		--		--
Phycoerythrin fluorescence/cell			++		++					
Primary production	+		++	++	--	++				
alpha				++		++				
Ik					--	++				
Growth rate										
- Total									-	
- <i>Prochlorococcus</i>								--		--
- <i>Synechococcus</i>			--						--	
- Picoeukaryote			--					--	--	
- Nanoeukaryote						+				
- Bacteria								++		++

860 *Estimated from flow cytometry

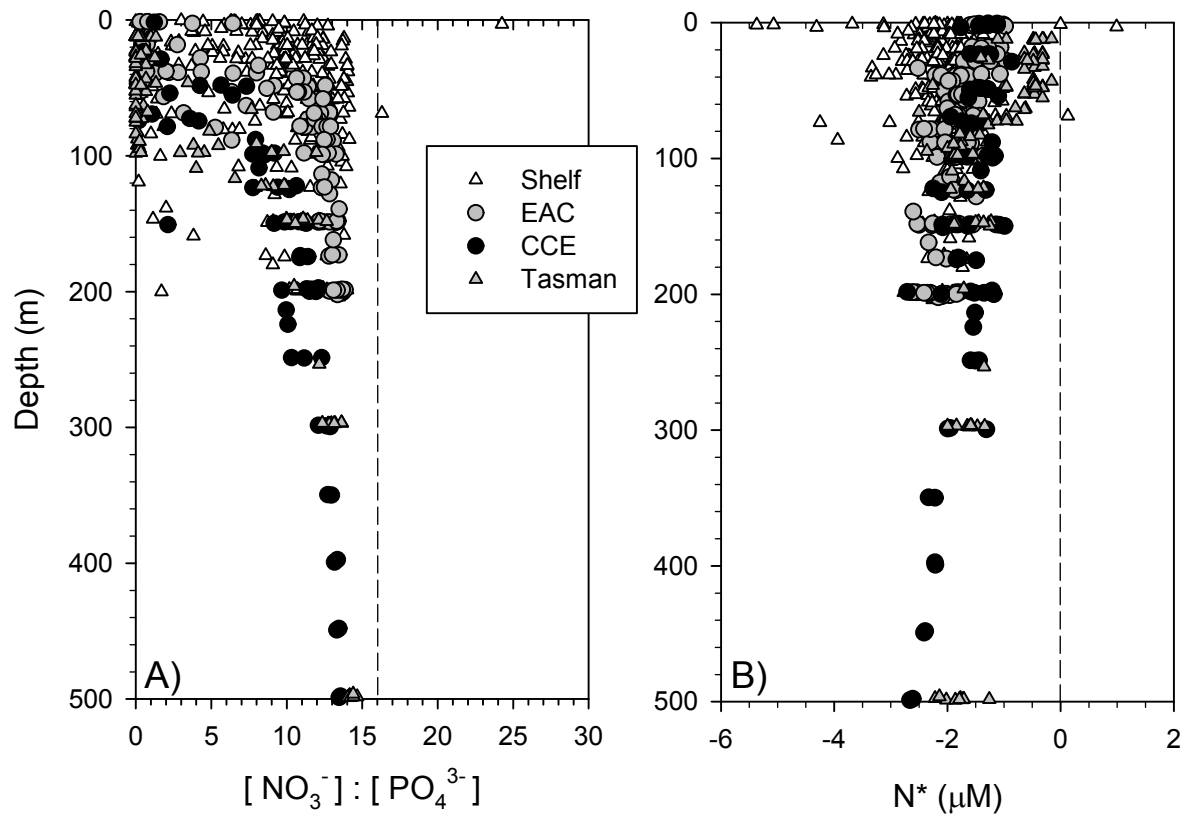
862 **Figures**

863



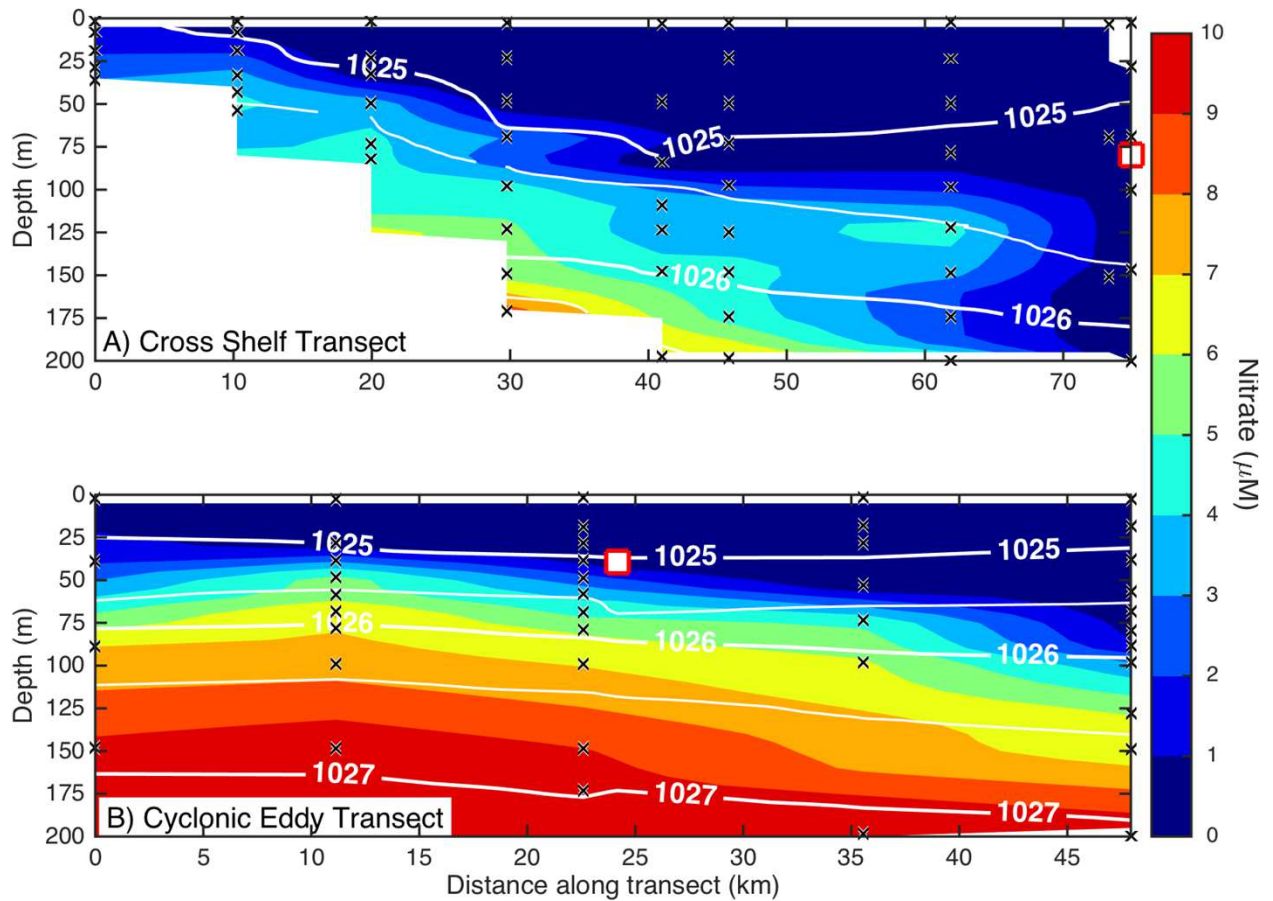
864

865 1. **Study area.** (A) Average sea surface temperature (SST) for October 2010 in the Tasman
 866 Sea, eastern Australia. The location of previous nutrient amendment studies are shown
 867 with symbols. The black box is the domain for the current study. (B) Average SST (20-
 868 25th October 2010) of the study domain during the voyage, showing location of sampling
 869 sites. The black line shows 200 m isobath, which approximates the continental shelf edge.
 870 Geostrophic velocities, estimated from sea-level anomaly are shown as arrows (20th
 871 October 2010).



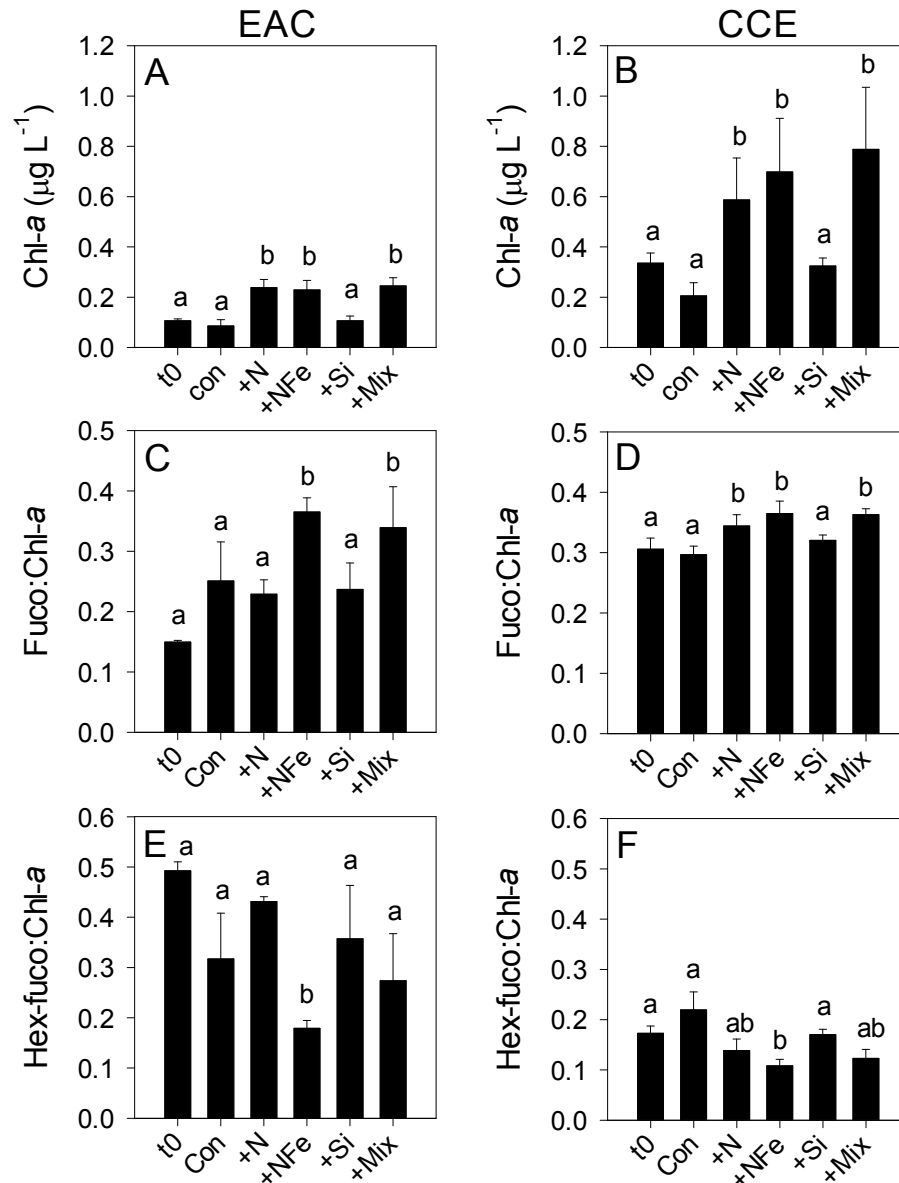
873
874
875
876
877
878
879

2. **Dissolved nitrogen pool relative to phosphorus.** The ratio of dissolved nitrate and phosphate (A) and nitrate deficit ($\text{N}^* = [\text{NO}_3^-] - 16[\text{PO}_4^{3-}]$) (B) in waters of the study domain, including the continental shelf (white triangles), East Australian Current (EAC; grey circles), cyclonic cold-core eddy (CCE; black circles) and Tasman Sea (grey triangles).



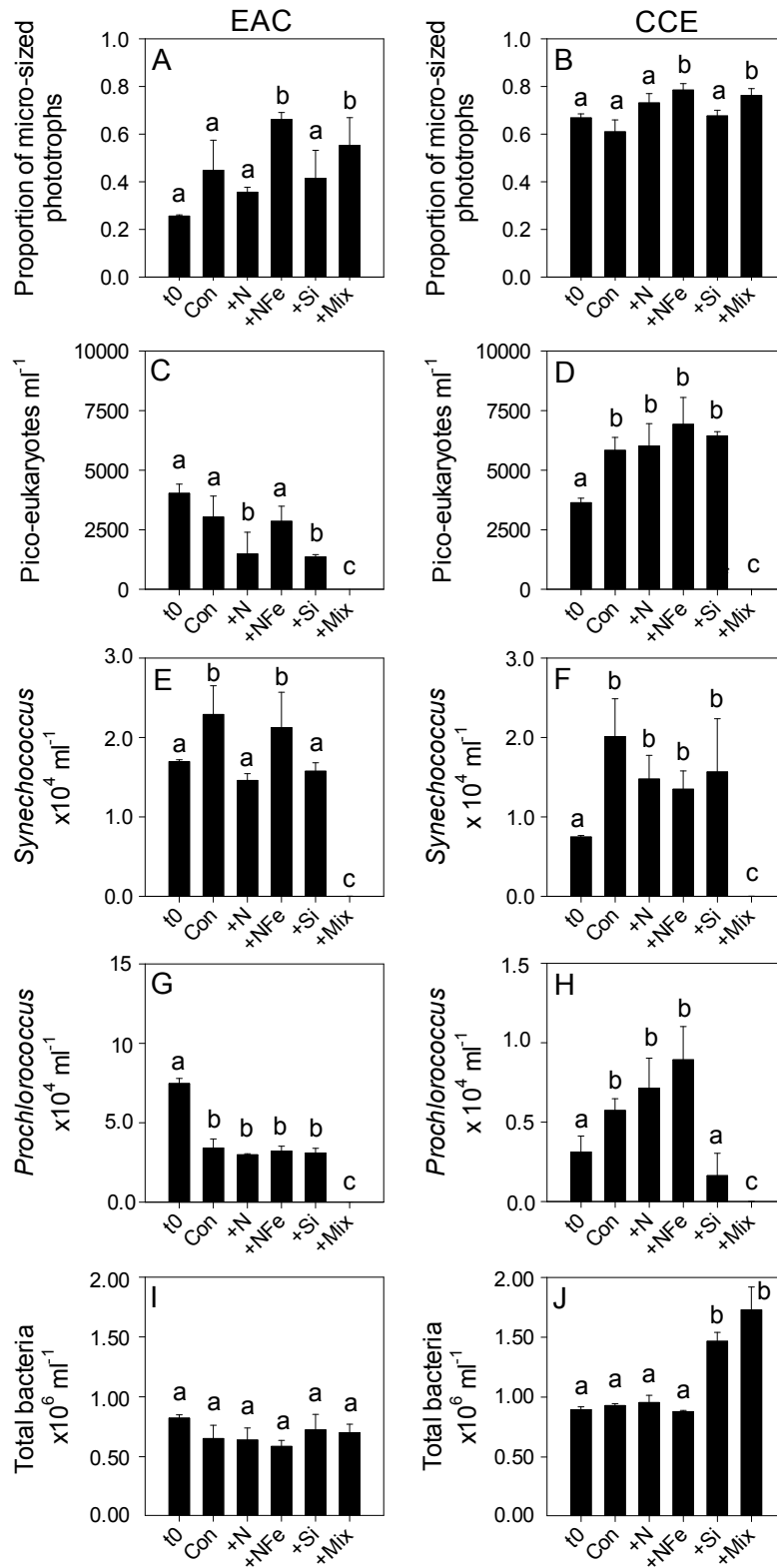
881
882
883
884
885
886
887

3. **Eddy influence on vertical nutrient distribution.** The distribution of dissolved nitrate (A) across the continental shelf to the East Australian Current, and (B) across the sampled cyclonic cold-core eddy. The white contours indicate seawater density, and the black crosses show the sampling locations for nitrate. The white squares indicate the water sampling locations for the nutrient amendment experiments.



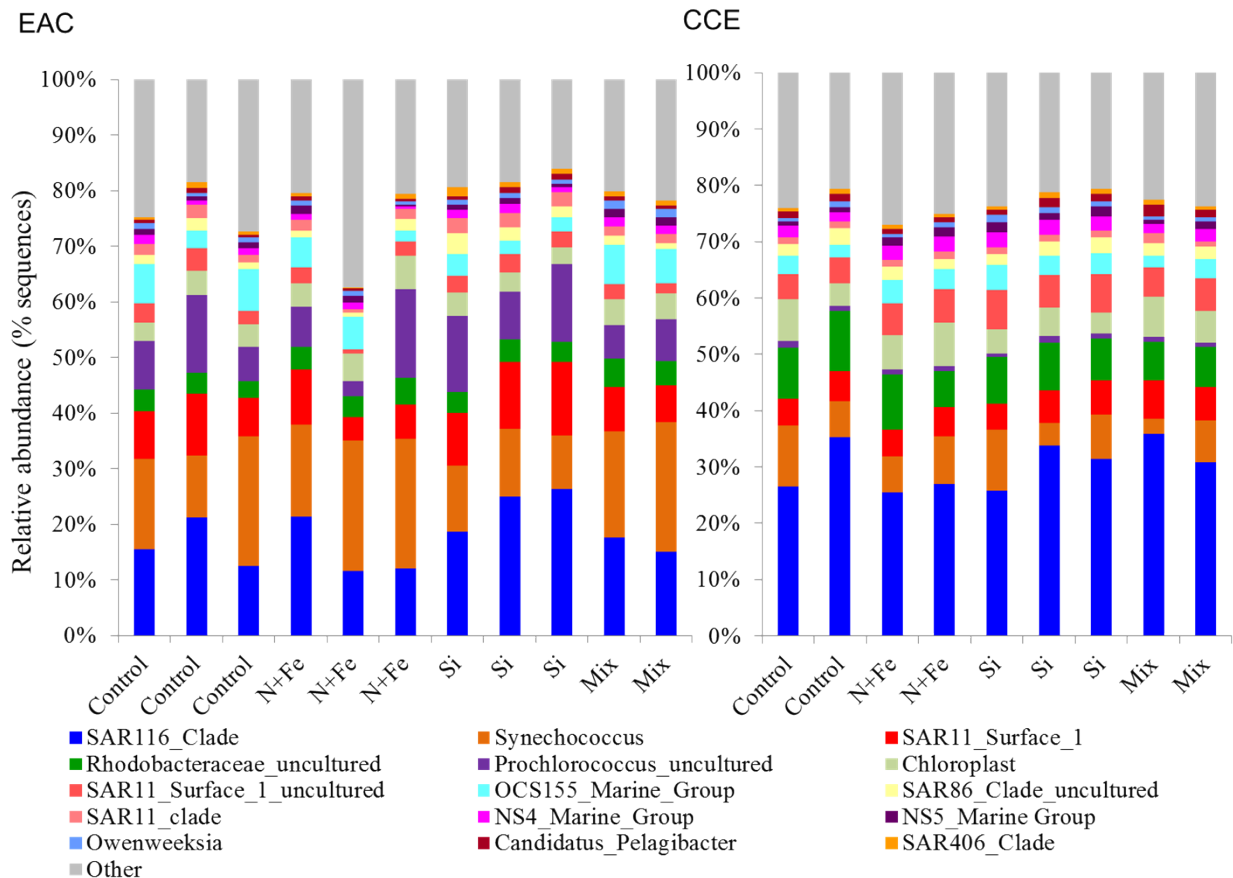
889
890
891
892
893
894
895
896
897
898
899
900
901

4. **Phototrophic responses to nutrient amendment.** Total Chl-a (monovinyl + divinyl), ratio of fucoxanthin to Chl-a and ratio of hex-fucoxanthin to Chl-a in the EAC (A, C and E, respectively) and CCE (B, D and F, respectively). These parameters are proxies for total phytoplankton biomass (Chl-a), relative biomass of diatoms (Fuco:Chl-a) and relative biomass of haptophytes (Hex-fuco:Chl-a). Treatments include initial (t0) and after 3 days nutrient amendment: Con = control, no amendment; +N = nitrate; +NFe = nitrate + iron; +Si = silicate; +Mix = nitrate + phosphate + silicate + iron. Values plotted are mean \pm standard deviation. Letters above bars indicate statistical differences amongst treatments (ANOVA, $\alpha = 0.05$) such that a is different to b, and ab is the same as a and b.



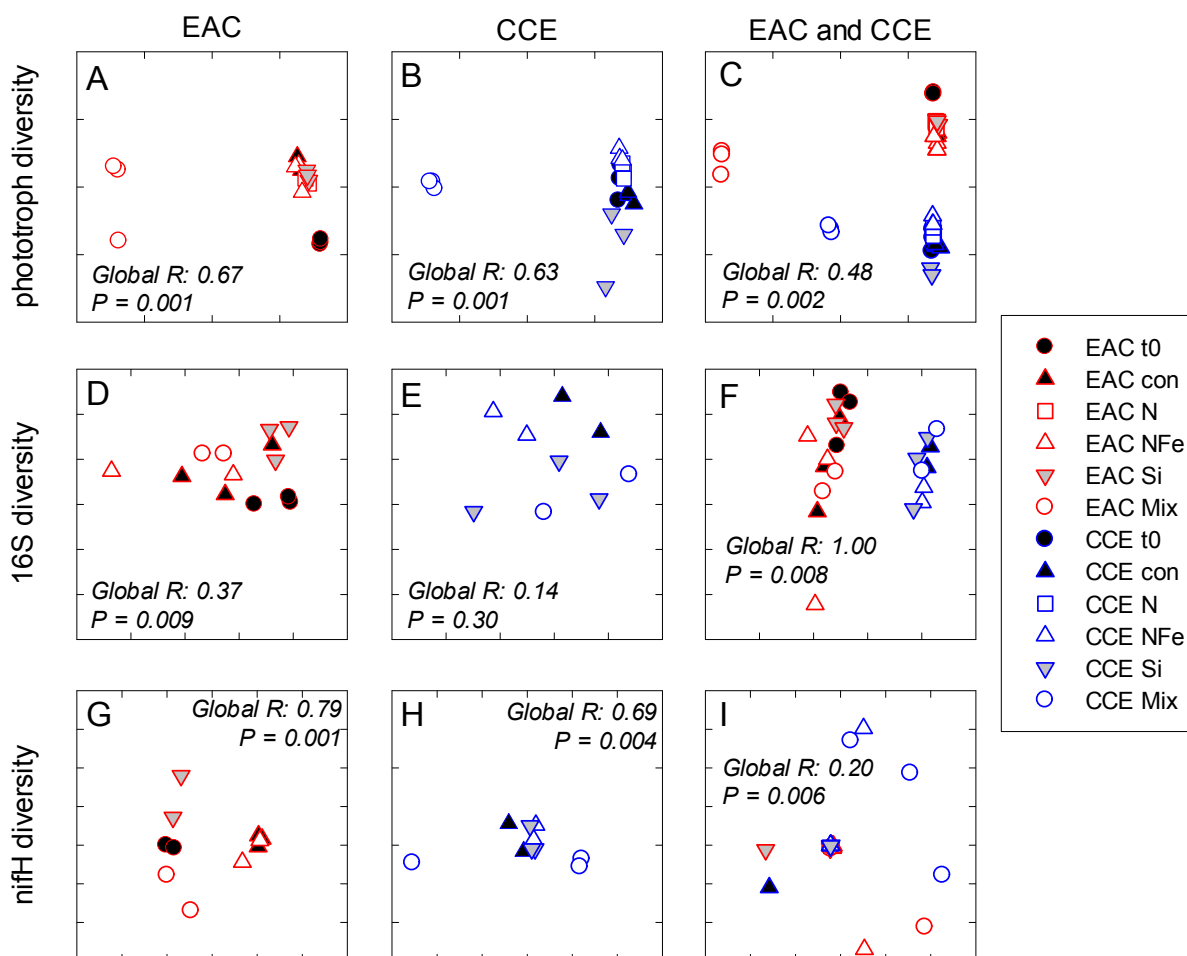
903
904

905 5. **Phototrophic and total bacteria responses to nutrient amendment.** Proportion of
 906 phototrophs larger than 20 μm in the EAC (A) and CCE (B), abundance of
 907 picoeukaryotes (C and D), abundance of *Synechococcus* (E and F), abundance of
 908 *Prochlorococcus* (G and H), and abundance of total bacteria (I and J). Treatments as in
 909 Figure 4. Values plotted are mean \pm standard deviation. Letters above bars indicate
 910 statistical differences amongst treatments (ANOVA, $\alpha = 0.05$) such that a is different to b
 911 and c.



912
 913 6. **Relative abundance of 16S rRNA operational taxonomic units.** Data are shown for
 914 sequences with $\geq 97\%$ sequence similarity to the SILVA database in the EAC (A) and
 915 CCE (B) amongst different treatments. For visual simplicity, only the top 15 OTUs are
 916 presented, with the upper grey bars representing the remaining 16S sequences detected.
 917 Control = no amendment; N+Fe = addition of nitrate and iron (10 μM and 1 nM,
 918 respectively), Si = addition of silicate (10 μM) and Mix = addition of nitrate, phosphate,
 919 silicate and iron (10 μM , 0.625 μM , 10 μM , 1 nM, respectively).

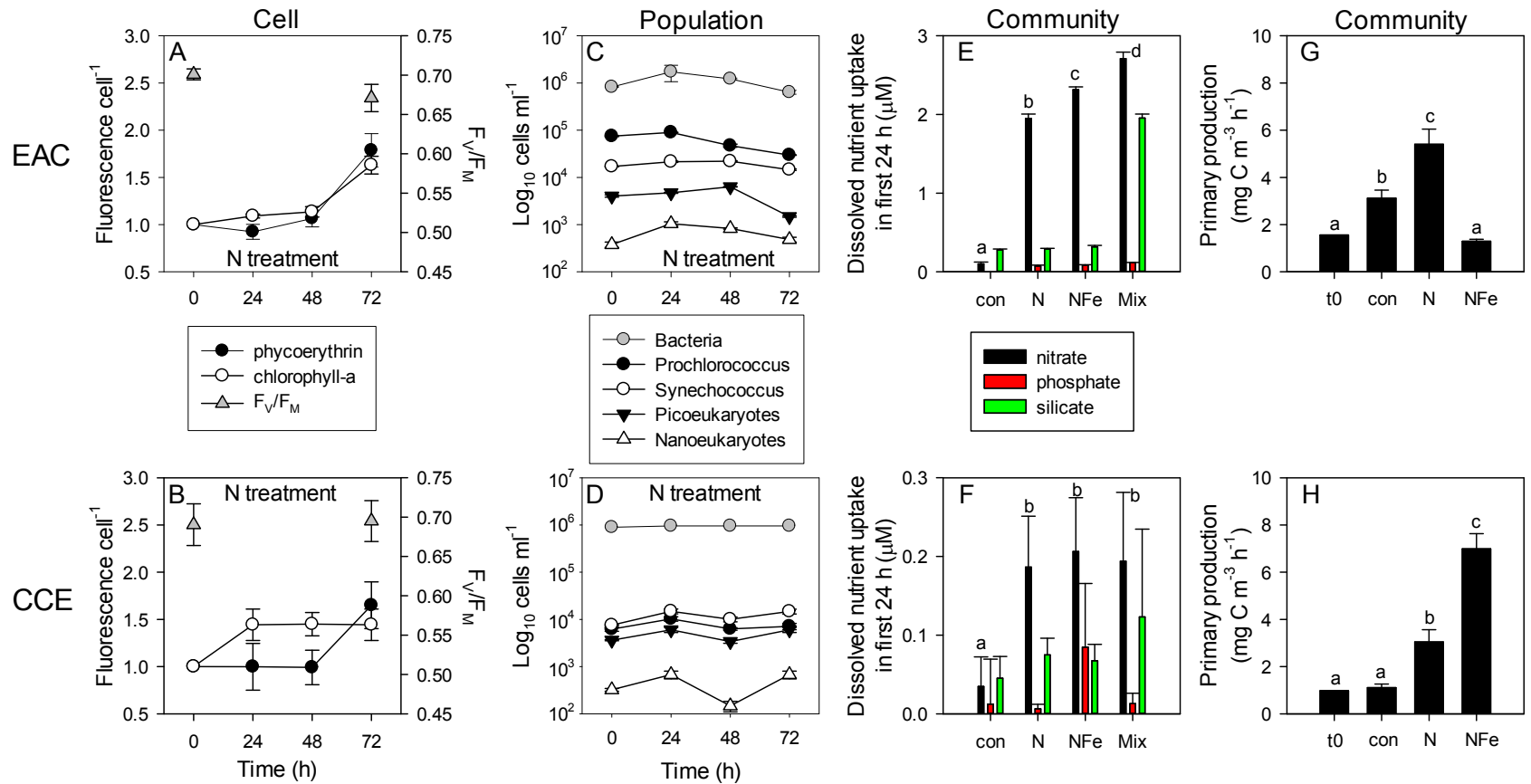
920
921
922
923



924
925

926 **7. Diversity of microbial communities.** Multi-dimensional Scaling (MDS) plots of
927 phototrophs (A,B and C), bacteria (D, E and F) and diazotrophs (G, H and I) in the East
928 Australian Current (EAC), cyclonic (cold-core) eddy (CCE) and both the EAC and CCE.
929 Clustering of samples is based on a Bray-Curtis similarity matrix of square-root
930 transformed HPLC pigment concentrations and flow cytometric counts of phototroph
931 abundance, Operational Taxonomic Units from 16S ribosomal genes or nitrogenase *NifH*
932 subunit genes. Plots on the same row have the same axes scales, to make them directly
933 comparable. Stress values for all plots are <0.10.

934

935
936
937

938 **8. Time-course of microbial responses to nutrient addition.** Daily Chl-a and phycoerythrin fluorescence in small pico-
 939 eukaryotes and *Synechococcus*, respectively under N amendment (A and B), together with photosynthetic efficiency (F_v/F_M) of
 940 the control phytoplankton assemblage at t₀ and t₇₂; Daily abundance of phototrophic and bacterial populations (C and D) in +N
 941 treatments in the EAC and CCE; Rate of macro-nutrient uptake in the first 24 h of incubation (E and F); Total carbon fixation
 942 by the phytoplankton assemblage in different treatments on day 3 (G and H). Values plotted are mean ± SD (n = 3) except for
 943 plots C and D which are mean ± SE (n = 3). Letters above bars indicate statistical differences amongst treatments (ANOVA, α
 944 = 0.05) such that a is different to b, c and d.

